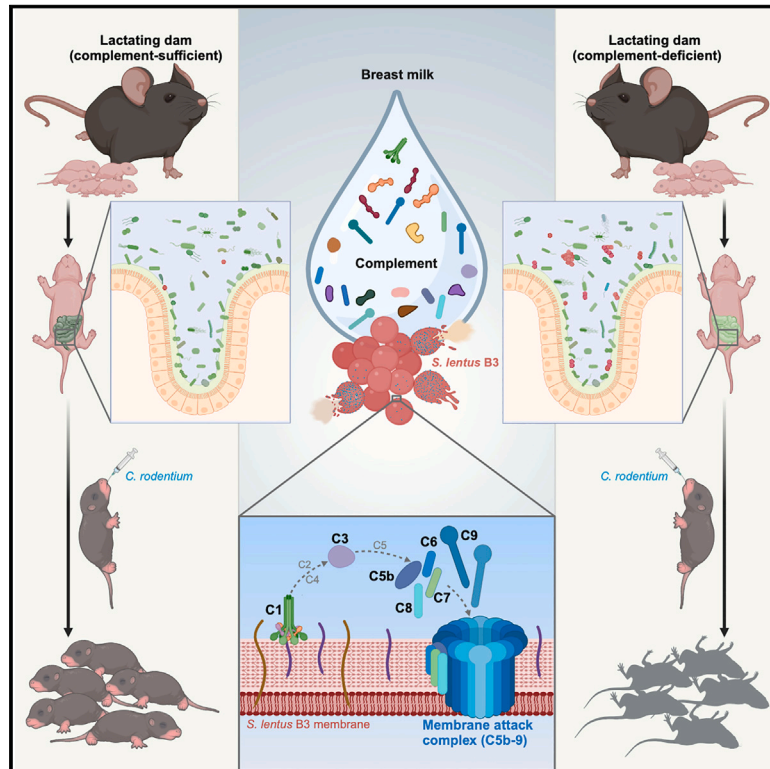


Complement in breast milk modifies offspring gut microbiota to promote infant health

Graphical abstract



Authors

Dongqing Xu, Siyu Zhou, Yue Liu,
Alan L. Scott, Jian Yang, Fengyi Wan

Correspondence

fwan1@jhu.edu

In brief

Breastfeeding offers evident benefits to infant health. This study finds that complement components in breast milk shape the offspring's evolving gut commensal microbiota, conferring protection against enteric infection.

Highlights

- Weanling mice with complement-deficient milk are susceptible to enteric infection
- Complement in milk selectively culls certain gram-positive microbes in the infant gut
- Breast milk complement is activated via a C1-dependent, antibody-independent pathway
- Early-life gut microbiota regulate neonate susceptibility to enteric infection



Article

Complement in breast milk modifies offspring gut microbiota to promote infant health

Dongqing Xu,¹ Siyu Zhou,² Yue Liu,¹ Alan L. Scott,^{1,3} Jian Yang,² and Fengyi Wan^{1,3,4,5,*}¹Department of Biochemistry and Molecular Biology, Bloomberg School of Public Health, Johns Hopkins University, Baltimore, MD, USA²NHC Key Laboratory of Systems Biology of Pathogens, National Institute of Pathogen Biology, Chinese Academy of Medical Sciences and Peking Union Medical College, Beijing, P.R. China³Department of Molecular Microbiology and Immunology, Bloomberg School of Public Health, Johns Hopkins University, Baltimore, MD, USA⁴Sidney Kimmel Comprehensive Cancer Center, Johns Hopkins University, Baltimore, MD, USA⁵Lead contact*Correspondence: fwan1@jhu.edu<https://doi.org/10.1016/j.cell.2023.12.019>

SUMMARY

Breastfeeding offers demonstrable benefits to newborns and infants by providing nourishment and immune protection and by shaping the gut commensal microbiota. Although it has been appreciated for decades that breast milk contains complement components, the physiological relevance of complement in breast milk remains undefined. Here, we demonstrate that weanling mice fostered by complement-deficient dams rapidly succumb when exposed to murine pathogen *Citrobacter rodentium* (CR), whereas pups fostered on complement-containing milk from wild-type dams can tolerate CR challenge. The complement components in breast milk were shown to directly lyse specific members of gram-positive gut commensal microbiota via a C1-dependent, antibody-independent mechanism, resulting in the deposition of the membrane attack complex and subsequent bacterial lysis. By selectively eliminating members of the commensal gut community, complement components from breast milk shape neonate and infant gut microbial composition to be protective against environmental pathogens such as CR.

INTRODUCTION

Despite the remarkable progress made in improving child health in recent decades, the reduction of neonate, infant, and child mortality remains a priority concern.¹ At birth, newborns are antigenically naive and thus lack effective adaptive immunity to most pathogenic challenges.² During the first weeks of life, neonates rely on innate immune mechanisms, the antibodies transferred from the mother during gestation, and the molecules and cells in breast milk to provide protection against microbial challenge and to set up a productive dialog with the infant's evolving microbiota.^{3–5} Clinical and experimental data strongly indicate that breastfeeding is effective in protecting newborns as breast milk not only provides high-quality nourishment but also confers a certain level of passive immunity by the transfer of immune cells and protective molecules that include antibodies, cytokines, antimicrobial peptides, and lactoferrin.^{6,7} Although bioactive components in breast milk can directly confer protection against selective pathogenic microbes,^{8–12} it is becoming increasingly clear that breast milk also has direct and indirect effects on infant health by exerting an influence on the compositional dynamics of the infant's rapidly evolving gut microbiota.^{13–15} Although the impact of breastfeeding on the development of a balanced gut microbiota has been estab-

lished,^{5,7} the relative contributions of the various immune cells and molecules remain to be defined.

The complement system is composed of more than 30 proteins found in the blood and interstitial fluids that, when activated, carry out a complex array of effector and regulatory functions,^{16–20} the best studied of which focus on host defense against microbial pathogens.²¹ Although initially described from the serum, where it makes up 10%–15% of the globulin fraction,²² the presence of complement components in breast milk has been noted from multiple mammalian species, including humans.^{23–26} Although a limited number of *in vitro* studies have examined whether the complement contained in breast milk has the capacity to mediate killing of pathogenic bacteria,^{27–29} the pathophysiological relevance of complement in breast milk is yet to be fully defined. One of the issues that has not been addressed is the possible contribution of complement components in breast milk in shaping the composition of the infant's gut microbiota and how this might influence susceptibility of newborns and infants to pathogenic microbes.

Here, we show that the mouse pups fostered by dams deficient in complement components in breast milk harbor an altered microbiota, which results in a failure to thrive and death upon challenge with the natural murine gut pathogen, *Citrobacter rodentium* (CR). Notably, the complement in breast

milk has the activity of directly lysing specific gram-positive commensal bacterial species via a C1-initiated, antibody-independent, and membrane attack complex (MAC)-dependent fashion. The selective killing of certain gram-positive species results in a gut microenvironment that protects the offspring from disease and death when challenged with CR. Our findings provide insights into how the complement contained in breast milk contributes to the establishment of a “protective” gut microbiota during the early stages of development and add to the list of the protective mechanisms of breast milk that promote infant health and defense against environmental pathogens.

RESULTS

Complement-deficient weanling mice are susceptible to enteric bacterial infection

The three pathways of complement activation, i.e., the classical pathway, the lectin pathway, and the alternative pathway, converge at the central step where C3 convertase activity is generated.^{16–18,30} To assess the impact of the complement system on host immune responses in infants against bacterial pathogens, weanling (21-day-old) wild-type (WT) C57BL/6J and complement component C3 knockout ($C3^{-/-}$) animals were challenged orally with CR at a dose that results in only minor reactions in WT animals.^{31–33} Although WT pups were only minimally affected in their growth (Figure 1A), expression of clinical signs (Figure 1B), and survival (Figure 1C) through 21 days post inoculation (dpi), CR infection of $C3^{-/-}$ pups caused significant decrements in growth and severe diarrhea by 7 dpi (Figures 1A and 1B), associated with >90% mortality (Figure 1C). The results suggested a key role for C3 and, by extension, the complement system in the protective response.

Of the three canonical pathways of C3 activation,^{34,35} the classical pathway of complement activation, which is initiated via the C1 complex,^{36–39} was studied first. The C1 complex is composed of 6 C1q, 2 C1r, and 2 C1s; each C1q molecule is composed of 6 heterotrimers made from C1qa, C1qb, and C1qc. The classical pathway is initiated by the C1 complex binding to antigen-bound immunoglobulin molecules or by C1 binding directly to the surface of microbes. A deletion of the gene encoding the C1qc chain ($C1qc^{-/-}$) blocks production of the heterotrimer and results in a functional C1 deficiency. At weaning and prior to CR challenge, WT, $C1qc^{-/-}$, and $C3^{-/-}$ animals had nearly identical body weights (Figure S1A). Despite almost identical CR colonization (Figure 1D), the $C1qc^{-/-}$ weanlings displayed the levels of attenuated growth, severe diarrhea, and lethality (Figures 1A–1C), observed in the $C3^{-/-}$ animals. The results suggested that C1-initiated activation was important for the protective effect of complement and, importantly, indicated that the lectin and alternative pathways (the other two mechanistic routes of C3 activation) played no or a minor role in the response. Therefore, our results supported the hypothesis that C3 activation via the C1-dependent cascade plays a critical role in infant defense against CR-induced lethality in weanling mice.

Morphological analysis revealed that the colons derived from CR-challenged $C1qc^{-/-}$ and $C3^{-/-}$ pups were markedly swollen and shortened compared with those from WT controls (Figures 1E and 1F). Histological analysis further illustrated the se-

vere colitis, characterized by crypt elongation, goblet cell depletion, and immune cell infiltration, in the colons of CR-challenged $C1qc^{-/-}$ and $C3^{-/-}$ animals (Figures 1G and 1H). In contrast, the colons from CR-challenged WT animals showed minimal histological evidence of pathology (Figures 1G and 1H). Additionally, live CR was detected in the liver and the spleen of CR-infected $C1qc^{-/-}$ and $C3^{-/-}$ animals, whereas these organs remained free of live bacteria in the WT controls (Figure 1I). Systemic dissemination of CR in the infected $C1qc^{-/-}$ and $C3^{-/-}$ groups indicated damage to the integrity of the colonic epithelial barrier, a notion that was supported by the substantially increased gut permeability in the $C1qc^{-/-}$ and $C3^{-/-}$ groups, as measured by leakage of gut-derived fluorescein isothiocyanate (FITC)-dextran to the serum (Figure 1J). Moreover, immunofluorescence staining demonstrated that CR predominantly attached to the luminal surface of the colonic epithelium in WT pups, whereas the CR in $C1qc^{-/-}$ and $C3^{-/-}$ animals penetrated the epithelial layer, even reaching the colonic crypts (Figure 1K). These results underscored the severe epithelial tissue damage that resulted from CR challenge in the absence of complement components C1 and C3.

Of note, the morphology, length, and histology of the colons derived from unchallenged WT, $C1qc^{-/-}$, and $C3^{-/-}$ weanling mice were comparable (Figures S1B–S1D). The intestinal epithelial permeability occurred at the low levels typically associated with intact barrier function and the livers and spleens were bacteria-free (Figures S1E–S1G). Moreover, CR challenge of WT, $C1qc^{-/-}$, and $C3^{-/-}$ adult (6- to 8-week-old) mice resulted in comparable increases in CR numbers in the gut, only transient body weight loss, and no mortality (Figures S1H–S1J). These mild symptoms observed in mature animals in response to CR challenge, as typically reported for WT adult mice during CR infection,^{31–33} suggested that the consequences of C1 or C3 deficiency is most impactful during the early stages of development, when breastfeeding provides critical passive protection against environmental exposure.

Complement in maternal milk is critical for infant susceptibility to CR

Although it has been appreciated for over five decades that complement components are present in colostrum and breast milk,^{24–26,40} the physiological relevance of this complement remains to be determined. Complement components were readily identified in the whey (the liquid after milk solids are removed) from WT C57BL/6J mice by mass spectrometry, and functional gene enrichment analysis illustrated that the “complement and coagulation cascades” was the top enriched pathway (Figure S2). To assess the potential relevance of complement in breast milk, we utilized a cross-fostering strategy to distinguish the relative contributions to the CR-induced phenotype made by breast milk and by the genetics of $C1qc^{-/-}$ and $C3^{-/-}$ weanlings. Both cross-fostered groups of $C1qc^{-/-}$ pups, which had comparable body weights at 21 days (Figures 2A and 2B), were separated from the dams and challenged with CR. Mirroring the findings in $C1qc^{-/-}$ weanling mice (Figures 1A–1C), $C1qc^{-/-}$ pups fostered by $C1qc^{-/-}$ dams succumbed to CR infection and exhibited decrements in growth and severe diarrhea (Figures 2C–2E). In striking contrast, all the $C1qc^{-/-}$ pups cross-fostered by WT dams survived the CR challenge, with no detectable decrease in growth

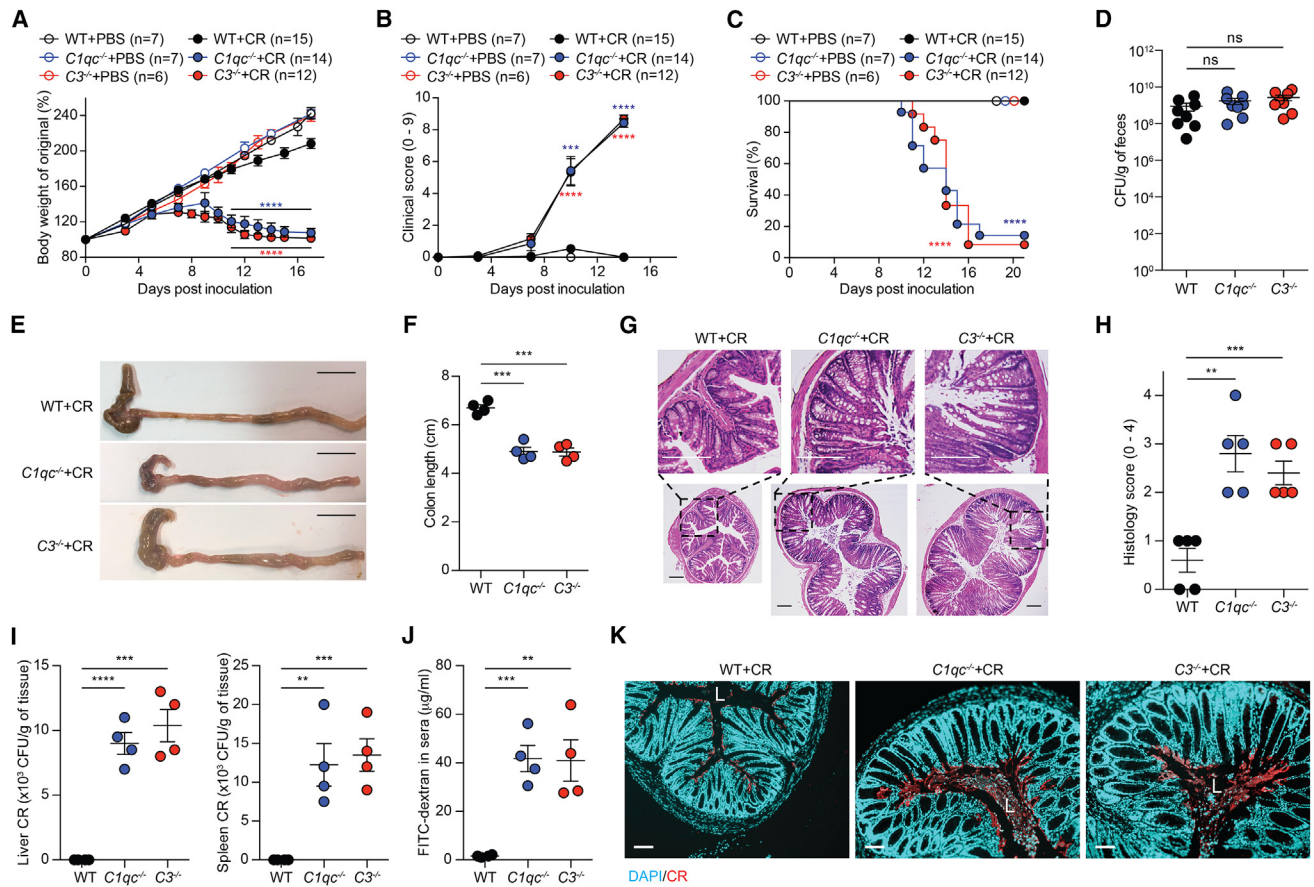


Figure 1. Complement-deficient pups are susceptible to *Citrobacter rodentium* infection

(A–C) Body weight changes (A), clinical scores (B), and survival (C) of 21-day-old wild-type (WT), *C1qc*^{-/-}, and *C3*^{-/-} mice at indicated days post inoculation (dpi) with 2×10^9 colony-forming units (CFUs) of *C. rodentium* (CR) or PBS vehicle control.

(D) Live CR recovered from the fecal samples of WT, *C1qc*^{-/-}, and *C3*^{-/-} pups at 7 dpi.

(E and F) Representative macrographs (E) and lengths (F) of the colon derived from CR-infected pups at 9 dpi. Scale bars, 1 cm.

(G and H) Hematoxylin and eosin staining (G) and histopathology scores (H) of colon sections derived from CR-challenged pups at 9 dpi. Scale bars, 200 μm.

(I) CR burdens in the liver (left) and the spleen (right) derived from CR-challenged pups at 9 dpi.

(J) FITC-dextran concentrations in the sera of CR-infected pups (9 dpi) at 4 h post oral administration of FITC-dextran.

(K) Representative immunofluorescence micrographs of CR in the colon derived from CR-infected pups at 9 dpi, with nuclei counterstained by DAPI. L, colonic lumen. Scale bars, 100 μm.

Data are mean ± SEM, with specific n numbers indicated. Data in (A)–(C) are combined results from at least three independent experiments; in (D)–(K) are representative results of at least two independent experiments. ns, not significant, ** p < 0.01, *** p < 0.001, and **** p < 0.0001, for *C1qc*^{-/-} versus WT in blue and *C3*^{-/-} versus WT in red, respectively.

See also Figure S1.

and minimal diarrhea (Figures 2C–2E). In addition, half of WT newborns were cross-fostered by *C1qc*^{-/-} dams, whereas the rest received milk lactated by the original WT dams prior to oral challenge with CR (Figure 2F). Although both groups of WT pups had comparable rates of growth through day 21 (Figure 2G), after CR challenge, WT dam-fostered WT pups continued to thrive, whereas cross-fostering by *C1qc*^{-/-} dams rendered WT pups highly susceptible to growth retardation, severe diarrhea, and distinctly elevated mortality rates (Figures 2H–2J). Similarly, WT and *C3*^{-/-} newborns were cross-fostered by *C3*^{-/-} and WT dams, respectively, with outcomes similar to those outlined above, i.e., fostering on WT dams was protective and fostering on *C3*-deficient dams made both WT and *C3*^{-/-} pups vulnerable

to CR-induced disease (Figures 2K–2T). These results demonstrate that complement-sufficient breast milk protects suckling mice from a CR-triggered lethal outcome.

To minimize possible additional microbiota-associated environmental variables beyond breast milk that influence these outcomes, we employed littermate and dam cohousing strategies. WT and *C1qc*^{-/-} female mice fostered by the same dams were cohoused since birth until delivering their pups; during lactation, WT and *C1qc*^{-/-} dams were cohoused to maximize their environmental similarity (Figure S3A). Consistently, fostering on WT dams was protective while fostering on *C1qc*^{-/-} dams resulted in pups, regardless of genotype, that were vulnerable to CR-induced growth retardation and lethality (Figures S3B and S3C). Moreover,

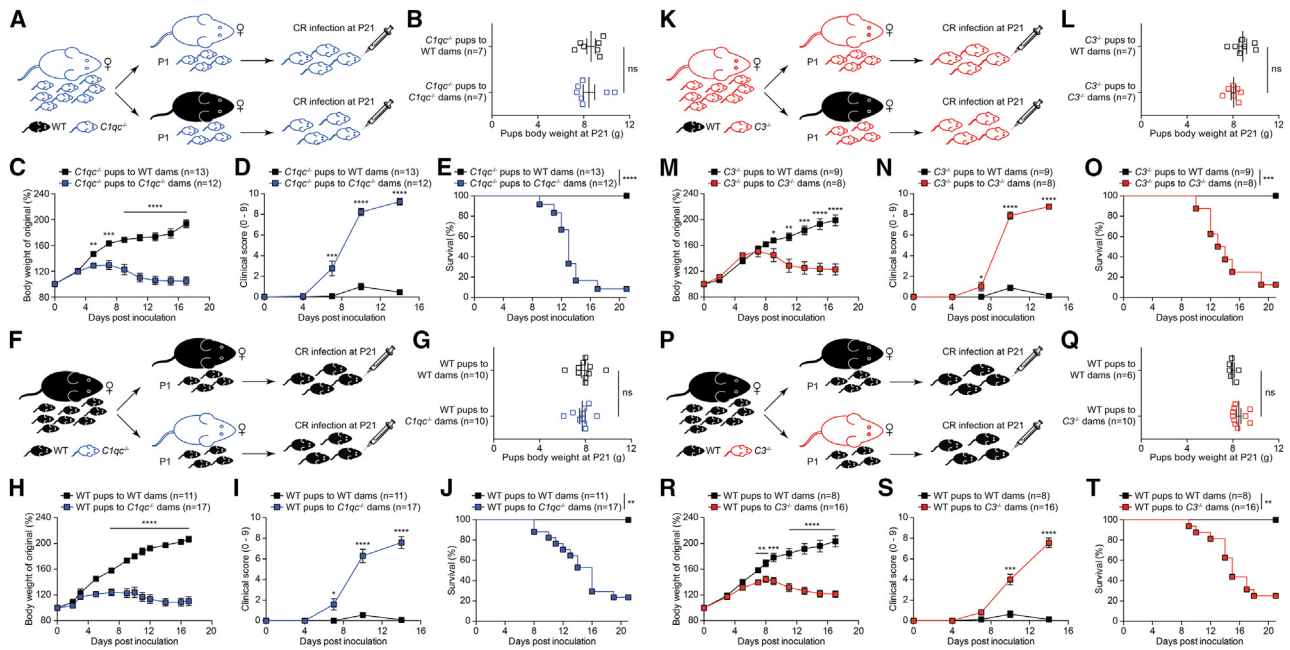


Figure 2. Complement in maternal milk protects weanling mice from CR-infection-caused growth faltering and lethality

(A and F) Experimental scheme of cross-fostering strategies. Wild-type (WT) C57BL/6J (black, filled) and *C1qc*^{-/-} (blue, open) breeding pairs were synchronized to generate pups born on the same day. *C1qc*^{-/-} (A) and WT (F) pups were divided into two groups on the day of birth and fostered by indicated dams. At post-natal day 21 (P21), the cross-fostered pups were weaned and orally inoculated with 2×10^9 CFUs of *C. rodentium* (CR).

(B and G) Body weight of the cross-fostered *C1qc*^{-/-} (B) and WT (G) pups at P21 prior to CR infection.

(C–E) Body weight changes (C), clinical scores (D), and survival (E) of the cross-fostered *C1qc*^{-/-} pups at indicated days post CR inoculation (dpi).

(H–J) Body weight changes (H), clinical scores (I), and survival (J) of the cross-fostered WT pups at indicated dpi.

(K and P) Experimental scheme of cross-fostering strategies. WT (black, filled) and *C3*^{-/-} (red, open) breeding pairs were synchronized to generate pups born on the same day. *C3*^{-/-} (K) and WT (P) pups were divided into two groups on the day of birth and fostered by indicated dams. At P21, the cross-fostered pups were weaned and orally inoculated with 2×10^9 CFUs of CR.

(L and Q) Body weight of the cross-fostered *C3*^{-/-} (L) and WT (Q) pups at P21 prior to CR infection.

(M–O) Body weight changes (M), clinical scores (N), and survival (O) of the cross-fostered *C3*^{-/-} pups at indicated dpi.

(R–T) Body weight changes (R), clinical scores (S), and survival (T) of the cross-fostered WT pups at indicated dpi.

Data are mean \pm SEM, with specific n numbers indicated. Data in (B)–(E), (G)–(J), (L)–(O), and (Q)–(T) are combined results from at least three independent experiments. ns, not significant; * $p < 0.05$, ** $p < 0.01$, *** $p < 0.001$, and **** $p < 0.0001$.

See also [Figures S2 and S3](#).

we obtained comparable results when WT and *C1qc*^{-/-} littermate dams were used in the same dam cohousing strategy ([Figures S3D–S3F](#)), indicating that the susceptibility of pups to CR challenge is largely or wholly determined by the presence of an intact complement system in breast milk.

Complement in breast milk alters microbiota composition, which contributes to CR-induced lethality

Breast milk plays an important role in establishing a balanced gut microbiota that indirectly protects against colonization by pathogens.^{7,8} To assess the impact of gut microbiota on the vulnerability of weanling animals to CR-induced disease, we rederived germ-free (GF) WT and *C1qc*^{-/-} mice for oral CR challenge. As expected, CR rapidly reached and sustained peak loads in weanling (21-day-old) GF WT and *C1qc*^{-/-} animals ([Figure 3A](#)). GF WT weanling mice were not vulnerable to CR challenge ([Figures 3B, 3C, and S4A–S4D](#)). Intriguingly, CR challenge failed to cause growth retardation, severe symptoms, or mortality in GF *C1qc*^{-/-} weanling mice ([Figures 3B and 3C](#)), mirroring the evi-

dence that the colonic morphology, lengths, and epithelial integrity derived from CR-challenged GF *C1qc*^{-/-} and WT weanling mice were all comparable ([Figures S4A–S4D](#)). Of note, transferring the cecal and colonic microbiota from 21-day-old specific-pathogen-free (SPF) WT mice to GF *C1qc*^{-/-} pups resulted in minimal impacts on growth, diarrheal symptoms, and survival after CR challenge ([Figures 3D–3G](#)). In contrast, the transfer of gut commensals from SPF *C1qc*^{-/-} rendered GF *C1qc*^{-/-} pups highly susceptible to CR challenge, with attendant decrements in growth, severe diarrhea, and distinctly elevated mortality rates ([Figures 3D–3G](#)). Shortened, swollen, and inflamed colons with substantially increased gut permeability were consistently observed in GF *C1qc*^{-/-} pups reconstituted with SPF *C1qc*^{-/-} gut commensals, but not in those reconstituted with SPF WT gut commensals ([Figures 3H, 3I, S4E, and S4F](#)). Moreover, GF WT pups reconstituted with SPF *C1qc*^{-/-} commensals became sensitive to CR challenge, while those that received SPF WT commensals remained resistant to CR infection ([Figures S4G–S4K](#)), mirroring their GF *C1qc*^{-/-} equivalents ([Figures 3D–3H](#)).

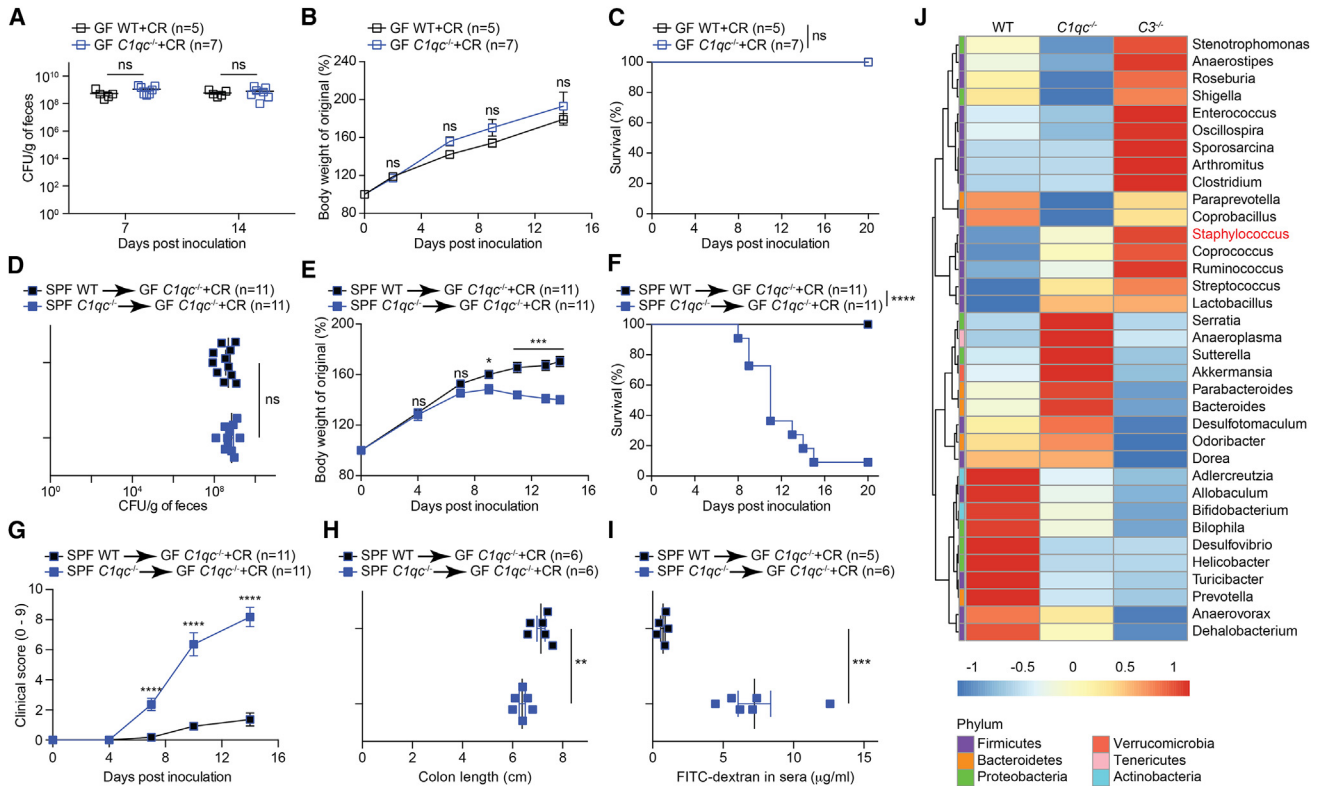


Figure 3. Gut microbiota in suckling mice plays a critical role in CR-infection-caused lethality

(A) Live *C. rodentium* (CR) recovered from the fecal samples of 21-day-old germ-free (GF) wild-type (WT) and *C1qc*^{-/-} mice at 7 and 14 days post inoculation (dpi) with 2 × 10⁹ CFUs of CR.

(B and C) Body weight changes (B) and survival (C) of 21-day-old GF WT and *C1qc*^{-/-} pups at indicated dpi with 2 × 10⁹ CFUs of CR.

(D) Live CR recovered from the fecal samples of 21-day-old GF *C1qc*^{-/-} pups, reconstituted at post-natal day 17 (P17) with the cecal and colonic microbiota derived from P21 specific-pathogen-free (SPF) WT or *C1qc*^{-/-} pups, at 7 dpi with 2 × 10⁹ CFUs of CR.

(E–G) Body weight changes (E), survival (F), and clinical scores (G) of 21-day-old GF *C1qc*^{-/-} pups, reconstituted and infected as in (D), at indicated dpi.

(H) Lengths of the colon derived from GF *C1qc*^{-/-} pups, reconstituted and infected as in (D), at 12 dpi.

(I) GF *C1qc*^{-/-} pups were reconstituted and infected as in (D). FITC-dextran concentrations in the sera of GF *C1qc*^{-/-} pups (12 dpi) at 4 h after oral administration of FITC-dextran.

(J) Species abundance heatmap of the dominant 35 genera detected using 16S rRNA gene-based high-throughput sequencing among the cecal and colonic contents derived from 21-day-old WT (n = 5), *C1qc*^{-/-} (n = 4), and *C3*^{-/-} (n = 5) pups.

Data are mean ± SEM, with specific n numbers indicated. Data in (A)–(C) are combined results from two independent experiments; in (D)–(G) are combined results from three independent experiments; in (H) and (I) are representative results of three independent experiments. ns, not significant; * p < 0.05, ** p < 0.01, *** p < 0.001, and **** p < 0.0001.

See also **Figures S4** and **S5**.

Together, these results implicate a crucial role for the composition of infant’s gut microbiota, shaped by the dam’s breast milk, in regulating susceptibility to CR-mediated severe disease in weanling animals.

The putative role of gut commensal microbiota in the susceptibility of suckling mice to CR-induced disease led us to profile the cecal and colonic microbiota in susceptible and refractory animals. Despite comparable numbers of observed species and similar levels of community richness and diversity (**Figures S5A–S5D**), 16S ribosomal RNA (rRNA) sequencing revealed that WT, *C1qc*^{-/-}, and *C3*^{-/-} weanling mice harbored gut microbiota with distinct overall compositions (**Figures 3J**, **S5E**, and **S5F**). Hence, it is possible that the dramatic difference observed in microbiota composition of WT, *C1qc*^{-/-}, and *C3*^{-/-}

weanling mice was a key factor in determining the susceptibility to CR infection.

Complement in breast milk eliminates gram-positive *Staphylococcus lentus* B3 in gut microbiota

The comparable body weights of WT, *C1qc*^{-/-}, and *C3*^{-/-} weanling mice, regardless of the complement status of the fostering dams (**Figures 2B**, **2G**, **2L**, **2Q**, and **S1A**), indicates that there were no substantial differences in the nutritional value of breast milk from WT, *C1qc*^{-/-}, or *C3*^{-/-} dams. Indeed, macronutrient content analyses revealed almost identical percentages of crude protein, crude fat, total sugar, water content, and calculated gross energy in breast milk collected from WT, *C1qc*^{-/-}, and *C3*^{-/-} dams (**Figures S6A–S6F**). Moreover, the protein concentrations

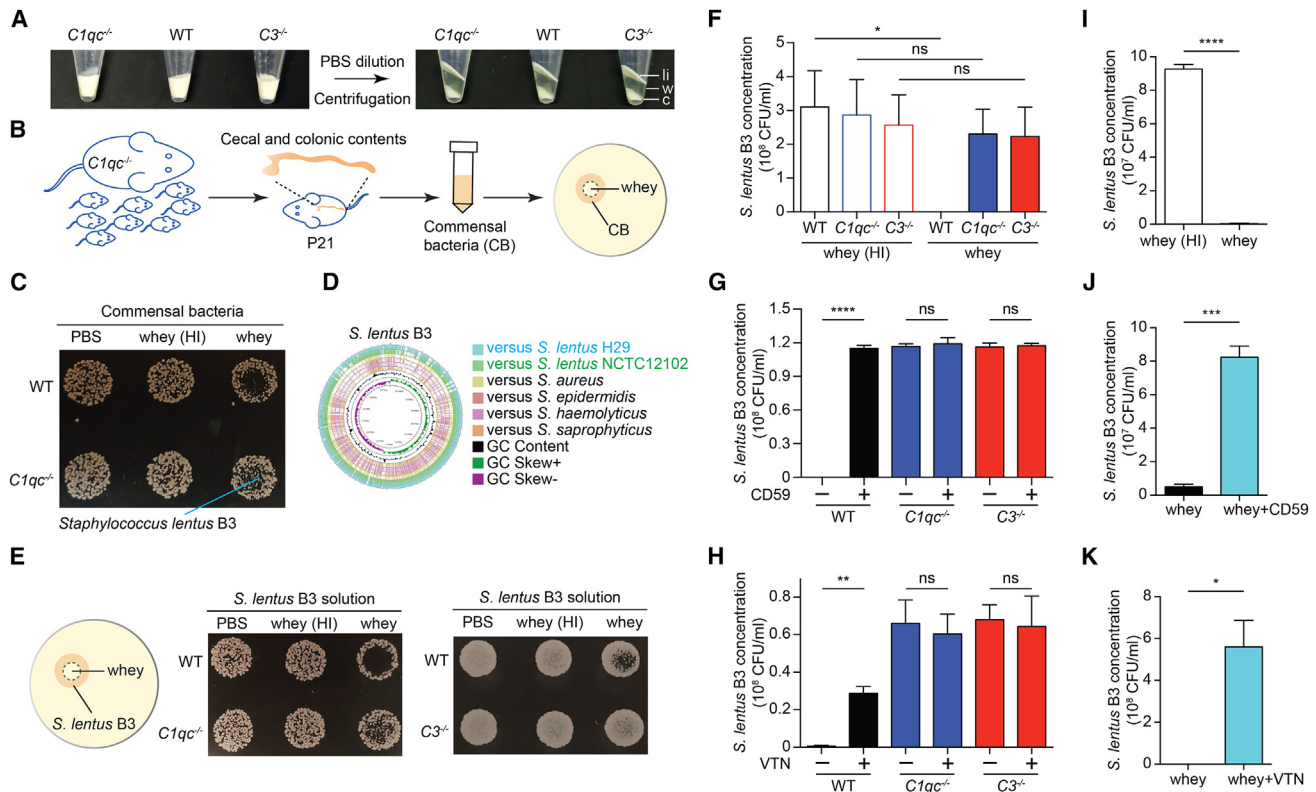


Figure 4. Breast milk complement kills gram-positive commensal bacterium *Staphylococcus lentus* B3

(A) Representative macrographs of the whole milk and whey (following PBS dilution and centrifugation) derived from wild-type (WT), *C1qc*^{-/-}, and *C3*^{-/-} dams. li, lipid; W, whey; C, casein.

(B) Experimental scheme of mouse whey bactericidal assays using cultivable commensal bacteria (CB) derived from *C1qc*^{-/-} pups at post-natal day 21 (P21).

(C) Representative macrographs of bactericidal assays on LB agar plates using WT and *C1qc*^{-/-} mouse whey to kill CB derived from *C1qc*^{-/-} pups, with PBS and heat-inactivated (HI) whey as negative controls. Indicated is one species, *Staphylococcus lentus* B3 strain, isolated from the cultivable CB of *C1qc*^{-/-} pups.

(D) A circular comparative genomic map of *S. lentus* B3 with other representative *Staphylococcus* genomes. From outer to inner, circles 1–6 show genomic comparisons in nucleotide level with *S. lentus* strains H29 and NCTC12102, *S. aureus* MW2, *S. epidermidis* RP62A, *S. haemolyticus* JCSC1435, and *S. saprophyticus* ATCC15305; circles 7 and 8 show G + C content and GC skew (G – C/G + C) of *S. lentus* B3 genome, respectively. The scale is given on the innermost circle.

(E) Representative macrographs of bactericidal assays on LB agar plates using the indicated mouse whey to kill *S. lentus* B3, with PBS and whey (HI) as negative controls. Left, experimental scheme.

(F–H) Whey bactericidal assays using *S. lentus* B3 cultured in LB medium, supplemented with whey derived from WT, *C1qc*^{-/-}, and *C3*^{-/-} dams and HI controls (F), or in the presence of CD59 (G) or vitronectin (VTN) (H). After 16-h culture with shaking, the indicated *S. lentus* B3 cultures were serially diluted and spotted on LB agar plates to determine CFUs. Shown are the concentrations of live *S. lentus* B3 in indicated LB media.

(I–K) Human whey bactericidal assays using *S. lentus* B3 cultured in LB medium, supplemented with regular or heat-inactivated (HI) human whey (I), or in the presence of CD59 (J) or VTN (K). After 16-h culture with shaking, the indicated *S. lentus* B3 cultures were serially diluted and spotted on LB agar plates to determine CFUs. Shown are the concentrations of live *S. lentus* B3 in indicated LB media.

Data are mean ± SEM and representative of three independent experiments. ns, not significant; * p < 0.05, ** p < 0.01, *** p < 0.001, and **** p < 0.0001. See also Figures S6–S11.

in the whey from WT, *C1qc*^{-/-}, and *C3*^{-/-} dams were comparable (Figures 4A, S6G, and S6H). Additionally, the levels of secretory antibodies, especially secretory immunoglobulin A (sIgA), which is reported to regulate the gut microbiota of infants,⁴¹ in the breast milk of WT, *C1qc*^{-/-}, and *C3*^{-/-} dams were all comparable (Figures S6I–S6N). This indicates that complement components, at least C1 and C3, do not impact the production of secretory antibodies in mouse breast milk. Hence, it seems unlikely that the levels of nutrients or immunoglobins provided by the lactating dams explain the striking differences in gut microbiota observed in WT, *C1qc*^{-/-}, and *C3*^{-/-} weanlings (Figure 3J).

The abundance of complement components in mouse whey (Figure S2) led us to examine whether complement directly or indirectly impacted the gut microbiota composition. The cecal and colonic bacteria from weanling *C1qc*^{-/-} pups were cultivated on Luria-Bertani (LB) agar plates; whey from WT or *C1qc*^{-/-} dams was spotted on top of the bacterial cultures (Figure 4B). Strikingly, the cultivable commensal bacteria were suppressed by the content of the whey from WT dams, but this inhibitory effect was substantially attenuated when the whey from *C1qc*^{-/-} dams was used (Figure 4C), suggesting that complement in mouse whey is involved in preventing the growth of

certain commensal bacterial species. Indeed, we characterized a cultivable isolate that was resistant to whey from $C1qc^{-/-}$ dams and identified it as *Staphylococcus lentus* (Figure S7A). We named this gram-positive bacterium *S. lentus* B3 (Figure 4C), the identification of which was further supported by the comparative genome analyses (Figures 4D and S7B). Likewise, similar findings were obtained when cecal and colonic bacteria from $C3^{-/-}$ weanlings were overlaid with whey from WT or $C3^{-/-}$ dams (Figures S7C and S7D). Of note, the abundance of *Staphylococcus* was markedly elevated in the gut microbiota of $C1qc^{-/-}$ and $C3^{-/-}$ pups compared with WT controls (Figure 3J), supporting the potential impact of complement in breast milk on selective bacteria (e.g., *S. lentus* B3) in the offspring's gut microbiota.

To assess the impact of *S. lentus* B3 on infant health under steady and infectious conditions, we performed *S. lentus* B3 monocolonization and simultaneous colonization of *S. lentus* B3 and CR in GF $C1qc^{-/-}$ pups. Similar to CR (Figures 3B, 3C, S8A, and S8B), *S. lentus* B3 inoculation alone did not affect the growth and survival of $C1qc^{-/-}$ pups (Figures S8A and S8B). In comparison to monocolonization, simultaneous colonization of *S. lentus* B3 and CR faintly, but significantly, attenuated the growth of GF $C1qc^{-/-}$ pups (Figure S8A), indicative of synergic *S. lentus* B3-CR interaction. Although not sufficient to cause mortality in GF $C1qc^{-/-}$ pups, the synergic interaction between *S. lentus* B3 and CR could substantially worsen the symptoms, which hints at the notion that *S. lentus* B3-CR interaction, in conjunction with other microbes in gut microbiota, contributes to the observed mortality in the CR-challenged SPF $C1qc^{-/-}$ pups (Figure 1). We then assessed whether reshaping the gut microbiota, especially eradicating *Staphylococcus* abundance in the pups receiving complement-deficient breast milk, could affect their susceptibility to CR infection. $C1qc^{-/-}$ pups fostered by the dams receiving maternal treatments with antibiotics vancomycin, neomycin, or cefoxitin in drinking water were still vulnerable to CR infection (Figures S8C and S8D). Interestingly, $C1qc^{-/-}$ dams administered a fenbendazole diet, a broad-spectrum benzimidazole commonly used in laboratory animals, completely rescued CR-infection-caused growth faltering and mortality in $C1qc^{-/-}$ pups, associated with dramatically reshaped gut microbiota, particularly reduced *Staphylococcus* levels, in $C1qc^{-/-}$ pups (Figures S8E–S8G). Likewise, $C3^{-/-}$ pups, fostered by $C3^{-/-}$ dams receiving fenbendazole treatment, fully reversed the vulnerability to CR infection and displayed substantially altered gut microbiota and attenuated *Staphylococcus* abundance (Figures S8H–S8J). Of note, eliminating *Staphylococcus* in the gut microbiota of $C1qc^{-/-}$ and $C3^{-/-}$ pups could avert their vulnerability to CR infection. Additionally, we analyzed the gut microbiota compositions of WT, $C1qc^{-/-}$, and $C3^{-/-}$ weaning pups (21-day-old) and adult mice (8-week-old). As expected, the numbers of observed species and community richness of bacterial families in the adult gut microbiota are remarkably higher than those in weaning pups (Figures S9A and S9B). Strikingly, in comparison with the high *Staphylococcus* abundance in $C1qc^{-/-}$ and $C3^{-/-}$ pups, *Staphylococcus* levels were comparably lower in WT, $C1qc^{-/-}$, and $C3^{-/-}$ adult mice (Figure S9C), which appears coincidentally correlated to their resistance to CR infection (Figures S1H–

S1J) Together, these results hint that *Staphylococcus* abundance in the mouse gut microbiota appears indicative of the susceptibility to CR infection.

To further characterize the effect of breast milk complement on *S. lentus* B3 abundance *in vivo*, we analyzed the microbiota compositions in the breast milk derived from nursing dams and in the stomach and small intestine of suckling pups, when the pups were at post-natal day 14 (P14). Interestingly, *Staphylococcus* appeared even higher in breast milk derived from WT dams compared with the $C1qc^{-/-}$ and $C3^{-/-}$ equivalents (Figure S10A), whereas *Staphylococcus* levels in the stomach of 14-day-old WT pups became slightly lower than those in $C1qc^{-/-}$ pups and profoundly lower than $C3^{-/-}$ pups (Figure S10B). Moreover, *Staphylococcus* abundance in the small intestine of $C1qc^{-/-}$ and $C3^{-/-}$ pups at P14 was also substantially elevated compared with WT pups (Figure S10C). These results are in line with our findings in the cecal and colon microbiota composition in P21 pups, where *Staphylococcus* levels were markedly elevated in $C1qc^{-/-}$ and $C3^{-/-}$ pups compared with WT controls (Figure 3J). Hence, complement in breast milk likely restrains *Staphylococcus* abundance prior to entering the small intestine, thus impacting the entire gut microbiota in pups.

Complement in breast milk directly kills *S. lentus* B3 via C1-initiated complement activation

Whey from WT dams readily hindered the growth of *S. lentus* B3 on LB agar plates or LB medium culture *in vitro*, whereas the bacterial growth was not inhibited by whey from $C1qc^{-/-}$ or $C3^{-/-}$ dams (Figures 4E and 4F). Moreover, heat-inactivated whey from WT, $C1qc^{-/-}$, or $C3^{-/-}$ dams failed to inhibit growth of *S. lentus* B3 (Figures 4E and 4F). The possible role of the complement MAC was explored using CD59, a glycoprotein that blocks the polymerization—and thus the pore-forming ability—of C9^{42,43} or vitronectin (VTN), a soluble factor that negatively regulates the formation of the C5b67 complex required for MAC formation.^{44,45} The addition of CD59 or VTN to the *in vitro* assays dampened the bacteria-suppressing capacity of whey from WT dams but had no impact on whey from $C1qc^{-/-}$ or $C3^{-/-}$ dams (Figures 4G and 4H).

The complement in human breast milk also displayed the capability to selectively suppress certain bacteria. Human whey derived from healthy donors hindered the growth of *S. lentus* B3 through a heat-labile mechanism (Figures 4I and S11A). The bacteria-suppressing capacity of human whey was substantially attenuated by CD59 (Figures 4J and S11B) and VTN (Figures 4K and S11C), supporting the involvement of MAC formation. Of note, time-kill kinetics assays further demonstrated bactericidal, rather than bacteriostatic, activities of human whey that were sensitive to CD59 or VTN (Figures S11D–S11F). These results point to a crucial role for an intact complement pathway in mouse and human breast milk for killing *S. lentus* B3.

The C1 complex is composed of a large subunit (C1q), which acts as a recognition protein or pathogen sensor, and two copies each of the inactive serine proteases C1r and C1s. When C1q binds directly to a pathogen/microbe surface or indirectly to antibodies bound to a pathogen, C1r is auto-activated and cleaves C1s to an active protease, which in turn cleaves the downstream

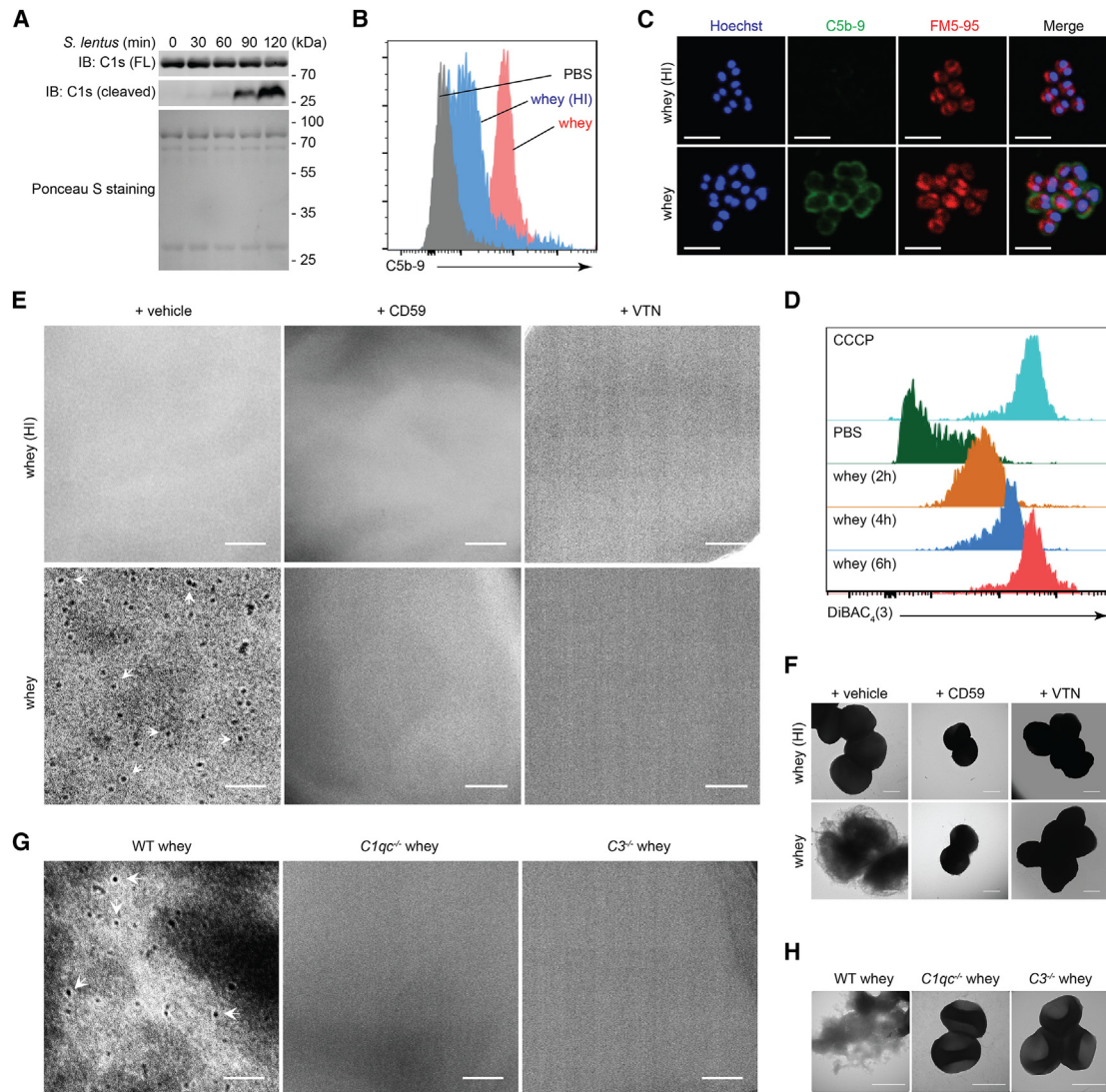


Figure 5. Complement in breast milk lyses *Staphylococcus lentus* B3 via C1 activation and MAC deposition

(A) Human whey and *Staphylococcus lentus* B3 were incubated for indicated time periods, followed by SDS-PAGE separation. The membrane was subjected to Ponceau S staining or immunoblot (IB) for full-length (FL) and cleaved C1s proteins.

(B) C5b-9 levels on *S. lentus* B3, following incubation with PBS, regular or heat-inactivated (HI) human whey, analyzed by flow cytometry.

(C) Representative immunofluorescence micrographs of C5b-9 on *S. lentus* B3 following incubation with indicated human whey, with DNA and membrane counterstained by Hoechst and FM5-95, respectively. Scale bars, 2 μ m.

(D) Representative histograms of DiBAC₄(3) fluorescence on *S. lentus* B3 incubated with PBS or human whey for indicated time periods, analyzed by flow cytometry, with the protonophore CCCP as a positive control.

(E and F) Representative cell membrane (E) and micrographs of bacterial morphology (F) of *S. lentus* B3 following incubation with indicated human whey in the presence and absence of CD59 or vitronectin (VTN). White arrows indicate the assembled ring-structured membrane attack complex (MAC) pores. Scale bars, 100 nm (E) and 500 nm (F).

(G and H) Representative cell membrane (G) and micrographs of bacterial morphology (H) of *S. lentus* B3 following incubation with whey derived from wild-type (WT), *C1qc*^{-/-}, and *C3*^{-/-} dams. White arrows indicate the assembled ring-structured MAC pores. Scale bars, 100 nm (G) and 500 nm (H).

Data in (A)–(G) are representative of three independent experiments.

See also Figure S12.

substrates C4 and C2. The proteolytic products of C4 and C2 combine to make a heterodimer with enzymatic activity that cleaves C3 (C3 convertase), a crucial step in the enzymatic cascade that leads to the eventual formation of the C5b-9 (MAC).^{46,47} Incubation of human whey and *S. lentus* B3 triggered

the cleavage of C1s (Figure 5A). In line with C1s activation, the terminal C5b-9 (MAC) was readily detected on the cell surface/membrane of *S. lentus* B3, when incubated with untreated, but not heat-inactivated, human whey (Figures 5B and 5C). Moreover, as measured by DiBAC₄(3), a negatively charged

fluorescent indicator widely used in evaluating bacterial membrane potential,⁴⁸ incubation with human whey disrupted the membrane potential of *S. lentus* B3 over time (Figure 5D). Of note, both CD59 and VTN substantially attenuated human-whey-mediated membrane potential loss in *S. lentus* B3 (Figures S12A and S12B). These results indicate that the C5b-9 (MAC) generated from the complement components in human whey can directly disrupt the membrane, leading to membrane depolarization in *S. lentus* B3. Indeed, transmission electron microscopy (TEM) revealed numerous MAC pores formed on the cell membrane of *S. lentus* B3, associated with damaged cell morphology, when incubated with human whey (Figures 5E and 5F). Moreover, MAC formation and *S. lentus* B3 cell membrane damage were significantly diminished by heat-inactivation of the whey or with the addition of CD59 or VTN (Figures 5E and 5F). Given C1s activation and the bactericidal activity of human whey (Figures 4I–4K and S11), these results suggest that human-whey-exposed *S. lentus* B3 was most likely killed via a C1-initiated pathway of complement activation resulting in terminal C5b-9 (MAC) deposition, similar to the killing documented for serum-derived complement for gram-negative *Escherichia coli*, *Salmonella minnesota*, and *Neisseria gonorrhoeae*.^{49–52} In contrast with *S. lentus* B3, incubation of human whey with gram-positive *S. aureus* SH1000 or gram-negative *E. coli* Nissle 1917 (*E. coli* N1917) failed to activate C1s or kill these bacteria (Figures S12C–S12F). Furthermore, as illustrated by TEM, *S. lentus* B3 incubated with WT mouse whey exhibited MAC pores in the bacterial cell membrane and lytic bacterial morphology; in contrast, no pore formation or altered cellular morphology was observed in the presence of *C1qc*^{−/−} or *C3*^{−/−} whey (Figures 5G and 5H). Hence, these results provide strong evidence that breast milk complement is activated in a C1-dependent cascade and leads to C5b-9 (MAC) deposition into the cell membrane of *S. lentus* B3, resulting in bacterial killing.

Activation of complement in the breast milk is independent of immunoglobulins

Of note, the cascade of complement activation can be initiated when the C1 complex either recognizes a microbial surface directly or binds to antibodies already bound to a pathogen.⁵³ To examine the role of antibodies in the bactericidal activity of complement in breast milk, we depleted immunoglobulin G (IgG) and immunoglobulin M (IgM) from human whey (Figure 6A). Strikingly, human whey depleted of IgG and IgM triggered C1s activation (Figure 6B), suggesting that antibodies are not required for the *S. lentus* B3-elicited complement activation. Incubation with the IgG- and IgM-depleted whey resulted in C5b-9 (MAC) deposition and cell-wall disruption in *S. lentus* B3 (Figures 6C–6E). To further validate that whey-derived *S. lentus* B3-elicited complement activation is antibody-independent, we employed whey from μ MT^{−/−} dams carrying a homozygous deletion of immunoglobulin heavy chain of the class μ , with global B cell deficiency⁵⁴ and absence of immunoglobulins of all isotypes (Figure 6F). Whey from μ MT^{−/−} and WT dams resulted in comparable C5b-9 (MAC) pores in the cell membrane and killing of *S. lentus* B3 (Figures 6G and 6H). Significantly, whey from μ MT^{−/−}*C1qc*^{−/−} dams failed to cause C5b-9 (MAC) formation

and cell damage in *S. lentus* B3 (Figures 6I and 6J). Taken together, these findings suggest an antibody-independent, C1-dependent pathway of complement activation leading to C5b-9 (MAC) deposition and bactericidal activity in human and mouse breast milk.

DISCUSSION

There is an increasing appreciation that the early-life progression in diversity and composition of the gut microbiota is a central contributing factor to human health and that imbalances in the gut microbial composition have short-term as well as far-reaching impacts on development and disease.^{55–57} However, the list of factors that contribute to the dynamics of microbiota development in newborns is still evolving. Breastfeeding, besides its well-documented role in providing high-quality nourishment for development and a source of key bacterial species important in establishing the early-life gut microbiota,^{8,58} contains important factors that directly and indirectly shape the infant's commensal microbiota.^{5,7,23} In particular, the multifaceted roles of antibodies in breast milk in conferring effective protection to offspring have been extensively investigated.⁵⁹ Although the presence of complement components in breast milk has been noted for decades, their physiological relevance has not been defined. Previous *in vitro* studies proposed that complement in breast milk has a bactericidal/bacteriostatic function against selective pathogens *E. coli* and *Helicobacter pylori*.^{28,29} In this study, we demonstrate that complement in mouse breast milk substantially modulates the early gut commensal community structure in offspring by selectively killing certain commensal bacteria, most notably the gram-positive bacteria *Staphylococcus*. Of note, *Staphylococcus* is among the first gut colonizers in human newborns during the first week after birth and exhibits declining population sizes in subsequent weeks. The reduction of *Staphylococcus* levels has been noted to coincide with the cessation of breastfeeding and consumption of solid food in humans.^{60,61} Consistently, *Staphylococcus* in mouse gut microbiota evidently shifts from higher abundance in infancy to declining levels in adulthood, which is likely due to the dietary transition from breast milk to formulated chow diet. It appears that during early life, *Staphylococcus* abundance in gut microbiota of weanling animals is correlated with the susceptibility to bacterial infection, and eliminating *Staphylococcus* averts their vulnerability to CR infection. These results highlight that complement components in breast milk could control *Staphylococcus* levels in the offspring's gut microbiota, which is crucial for newborns and infant health. Moreover, complement-mediated bactericidal activity targeting the isolated *Staphylococcus lentus* B3 strain is conserved between mouse and human breast milk. Overall, our findings suggest that, beyond controlling pathogens, complement in breast milk possess an evolutionally conserved capacity to eliminate selective commensal microbes, thus functioning in shaping the gut microbiota during the early stages of development.

We show that complement components C1q and C3 are pivotal for the bactericidal activity of breast milk complement to *S. lentus* B3. In particular, the C5b-9 (MAC), which is the terminal effector complex of complement activation, is assembled

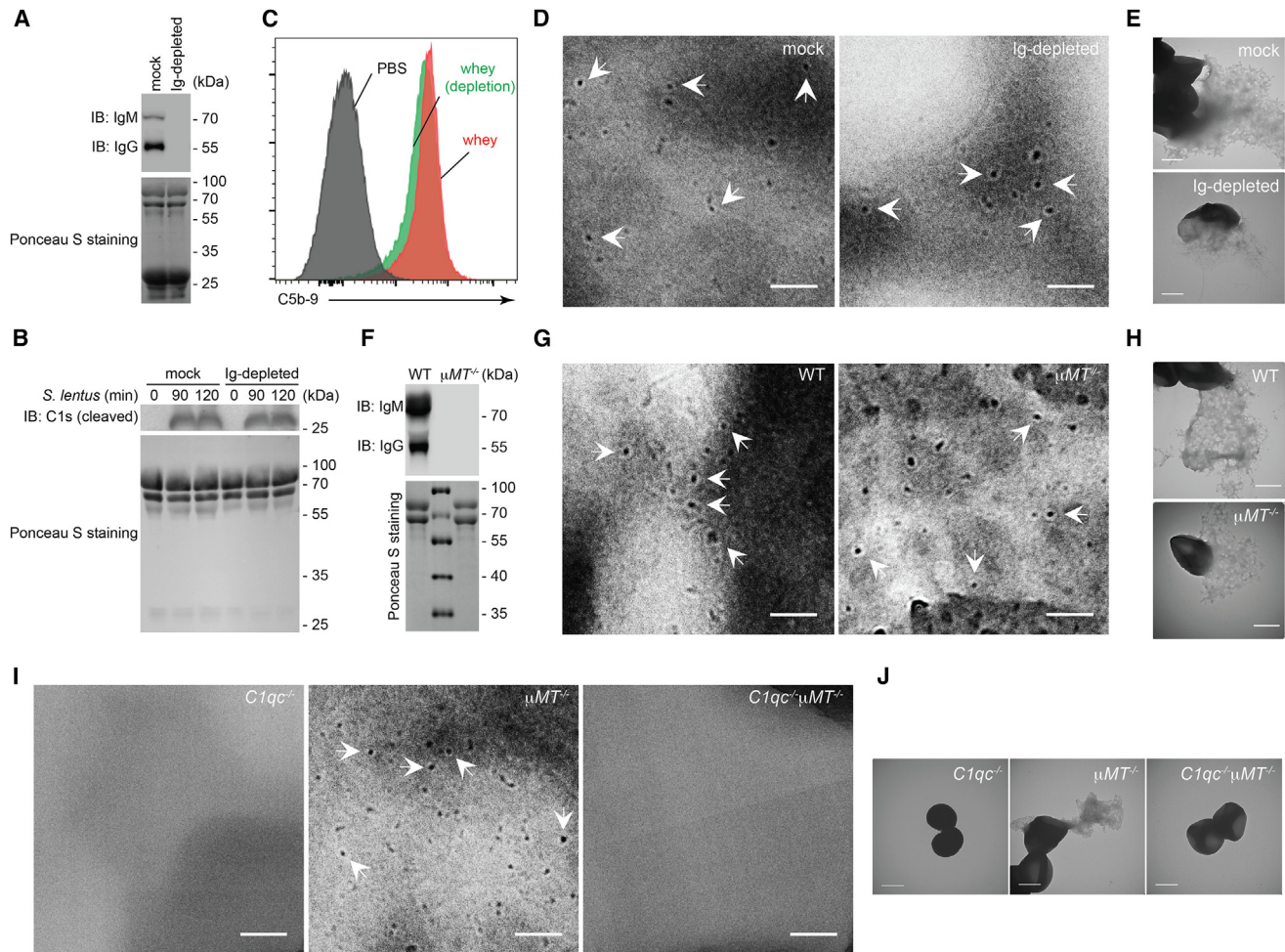


Figure 6. Complement in breast milk kills *Staphylococcus lentus* B3 antibody-independently

(A) Immunoglobulin G (IgG) and IgM-depleted (Ig-depleted) and mock-treated human whey samples were SDS-PAGE separated, followed by Ponceau S staining or immunoblot (IB) for IgM and IgG.
 (B) Mock-treated and Ig-depleted human whey, incubated with *Staphylococcus lentus* B3 for indicated time periods, were SDS-PAGE separated, followed by Ponceau S staining or IB for activated C1s proteins.
 (C) C5b-9 levels on *S. lentus* B3, following incubation with PBS or indicated human whey, analyzed by flow cytometry.
 (D and E) Representative cell membrane (D) and micrographs of bacterial morphology (E) of *S. lentus* B3 following incubation with indicated human whey. White arrows indicate the assembled ring-structured membrane attack complex (MAC) pores. Scale bars, 100 nm (D) and 500 nm (E).
 (F) Whey derived from wild-type (WT) C57BL/6J and $\mu MT^{-/-}$ dams was SDS-PAGE separated, followed by Ponceau S staining or IB for IgM and IgG.
 (G–J) Representative cell membrane (G) and (I) and micrographs of bacterial morphology (H) and (J) of *S. lentus* B3 following incubation with whey derived from indicated dams. White arrows indicate the assembled ring-structured MAC pores. Scale bars, 100 nm (G and I) and 500 nm (H and J).
 Data in (A)–(J) are representative of three independent experiments.

onto the cell membrane of *S. lentus* B3 and leads to the loss of membrane potential as well as cell damage and lysis. It was previously reported that when some gram-positive bacteria are exposed to human serum, C5b-9 (MAC) deposition can be observed but does not lead to bacterial killing.⁶² Distinct from serum complement, when gram-positive *S. lentus* B3 is exposed to breast milk, the readily detected C5b-9 (MAC) deposition does result in *S. lentus* B3 cell lysis, thus harboring bactericidal activity. The cascade of complement activation is canonically initiated by an antibody-dependent mechanism that involves C1q_{r2s2} complex binding to the anti-bacterial IgM or IgG bound to anti-

genic determinants found on the surface of the microbe.⁶³ Also, the initiation of complement activation can be achieved when C1q directly recognizes a microbial surface, supported by previous evidence from *in vitro* studies that, in the absence of an antibody, serum-derived C1q can bind directly to the surface of a few gram-negative bacteria^{64–68} or purified surface components of gram-positive bacteria.^{69,70} In this study, antibody-deficient whey does not impact the C1s activation in response to *S. lentus* B3, formation of C5b-9 (MAC) pores on *S. lentus* B3, and bacterial killing. These results strongly support the notion that, in breast milk, the cascade of complement

activation is initiated in an antibody-independent manner to kill certain gram-positive microbes in the infant's gut microbiota; such selective microbial killing protects the gut from colonization later in life by pathogenic microbes such as CR. Together, our findings demonstrate that complement in breast milk plays a critical role in the development and establishment of a health-promoting early-life gut microbiota and adds to the mechanisms by which breastfeeding confers protection and promotes infant health.

Limitations of the study

Complement in breast milk selectively eliminates certain commensal bacteria, thus modifying the gut microbiota composition in weanling mice. Although the role of *S. lentus* B3 is illustrated here, it is likely that other commensal microbes also contribute to promoting infant health. Further investigations are needed to identify additional microbes similarly eliminated via the antibody-independent action of breast milk complement, which would facilitate studies to define the molecular basis for antibody-independent C1q-microbe interactions that lead to complement activation. Complement in breast milk kills gram-positive *S. lentus* B3 directly via C5b-9 (MAC) pore formation, whereas the C5b-9 (MAC) deposition during serum or recombinant complement activation does not kill gram-positive bacteria. It warrants further investigation whether additional bioactive component(s) in breast milk may participate in the complement-mediated lysis of gram-positive bacteria. Littermate and dam cohousing strategies eliminate most possible environmental variables in the experiments performed here using complement global knockout animals. It would be of interest to develop tissue-specific complement conditional knockout mice for studies on breast milk complement biology.

STAR★METHODS

Detailed methods are provided in the online version of this paper and include the following:

- **KEY RESOURCES TABLE**
- **RESOURCE AVAILABILITY**
 - Lead contact
 - Materials availability
 - Data and code availability
- **EXPERIMENTAL MODEL AND STUDY PARTICIPANT DETAILS**
 - Animals
 - Microbe strains
 - Human breast milk samples
- **METHOD DETAILS**
 - Cross-fostering experiments
 - Reconstitution of GF mice with SPF commensal microbiota
 - Bacterial infection in mice
 - Histology and immunofluorescence
 - FITC-dextran assays
 - Flow cytometry and confocal microscopy
 - Microbiota composition
 - Collection of breast milk whey

- Mass spectrometry and protein functional annotation
- Immunoblot
- Breast milk bactericidal assays
- Whole genome sequencing, genome assembly, and comparative analysis
- Enzyme-linked immunosorbent assays
- Maternal antibiotics treatment
- Membrane depolarization
- Immunoglobulin depletion in human milk whey
- Transmission electron microscopy

● QUANTIFICATION AND STATISTICAL ANALYSIS

ACKNOWLEDGMENTS

We appreciate S. Lajoie and M. Mugnier for sharing mouse strains; N. Archer and T. Danino for sharing bacterial strains; M. Power for measuring milk macronutrients; H. Ding, R. Cole, and B. Smith for facilitating the studies using germ-free animals, mass spectrometry, and electron microscopy, respectively; C. Sears for sharing reagents; and Mother's Milk Bank for providing human milk samples. This work was supported in part by grants from National Institutes of Health (GM111682, AI137719, and CA244350 to F.W.); Department of Defense (W81XWH-19-1-0479 to F.W.); American Association of Immunologists (Career in Immunology Fellowship to D.X.); and American Heart Association (19PRE34380234 to Y.L.). The funders had no role in study design, data collection and analysis, decision to publish, or preparation of the manuscript.

AUTHOR CONTRIBUTIONS

Conceptualization, F.W.; methodology, F.W. and D.X.; investigation, D.X.; software, S.Z. and J.Y.; resources, Y.L. and A.L.S.; writing – original draft, F.W. and D.X.; writing – review & editing, all authors; supervision, F.W.; funding acquisition, F.W.

DECLARATION OF INTERESTS

The authors declare no competing interests.

Received: September 30, 2022

Revised: October 3, 2023

Accepted: December 14, 2023

Published: January 18, 2024

REFERENCES

1. Perin, J., Mulick, A., Yeung, D., Villavicencio, F., Lopez, G., Strong, K.L., Prieto-Merino, D., Cousens, S., Black, R.E., and Liu, L. (2022). Global, regional, and national causes of under-5 mortality in 2000–19: an updated systematic analysis with implications for the Sustainable Development Goals. *Lancet Child Adolesc. Health* 6, 106–115.
2. Basha, S., Surendran, N., and Pichichero, M. (2014). Immune responses in neonates. *Expert Rev. Clin. Immunol.* 10, 1171–1184.
3. Camacho-Morales, A., Caba, M., García-Juárez, M., Caba-Flores, M.D., Viveros-Contreras, R., and Martínez-Valenzuela, C. (2021). Breastfeeding contributes to physiological immune programming in the newborn. *Front. Pediatr.* 9, 744104.
4. Hurlley, W.L., and Theil, P.K. (2011). Perspectives on immunoglobulins in colostrum and milk. *Nutrients* 3, 442–474.
5. Fehr, K., Moossavi, S., Sbihi, H., Boutin, R.C.T., Bode, L., Robertson, B., Yonemitsu, C., Field, C.J., Becker, A.B., Mandhane, P.J., et al. (2020). Breastmilk feeding practices are associated with the co-occurrence of bacteria in mothers' milk and the infant gut: the CHILD cohort study. *Cell Host Microbe* 28, 285–297.e4.
6. Hanson, L.A., and Korotkova, M. (2002). The role of breastfeeding in prevention of neonatal infection. *Semin. Neonatol.* 7, 275–281.

7. Le Doare, K., Holder, B., Bassett, A., and Pannaraj, P.S. (2018). Mother's milk: a purposeful contribution to the development of the infant microbiota and immunity. *Front. Immunol.* **9**, 361.
8. Lyons, K.E., Ryan, C.A., Dempsey, E.M., Ross, R.P., and Stanton, C. (2020). Breast milk, a source of beneficial microbes and associated benefits for infant health. *Nutrients* **12**, 1039.
9. Harris, N.L., Spoerri, I., Schopfer, J.F., Nembrini, C., Merky, P., Massacand, J., Urban, J.F., Jr., Lamarre, A., Burki, K., Odermatt, B., et al. (2006). Mechanisms of neonatal mucosal antibody protection. *J. Immunol.* **177**, 6256–6262.
10. Zheng, W., Zhao, W., Wu, M., Song, X., Caro, F., Sun, X., Gazzaniga, F., Stefanetti, G., Oh, S., Mekalanos, J.J., et al. (2020). Microbiota-targeted maternal antibodies protect neonates from enteric infection. *Nature* **577**, 543–548.
11. Gopalakrishna, K.P., Macadangdang, B.R., Rogers, M.B., Tometich, J.T., Firek, B.A., Baker, R., Ji, J., Burr, A.H.P., Ma, C., Good, M., et al. (2019). Maternal IgA protects against the development of necrotizing enterocolitis in preterm infants. *Nat. Med.* **25**, 1110–1115.
12. Erickson, J.J., Archer-Hartmann, S., Yarawsky, A.E., Miller, J.L.C., Seveau, S., Shao, T.Y., Severance, A.L., Miller-Handley, H., Wu, Y., Pham, G., et al. (2022). Pregnancy enables antibody protection against intracellular infection. *Nature* **606**, 769–775.
13. Bäuml, A.J., and Sperandio, V. (2016). Interactions between the microbiota and pathogenic bacteria in the gut. *Nature* **535**, 85–93.
14. Kåhrström, C.T., Pariente, N., and Weiss, U. (2016). Intestinal microbiota in health and disease. *Nature* **535**, 47.
15. Kim, Y.G., Sakamoto, K., Seo, S.U., Pickard, J.M., Gilliland, M.G., 3rd, Puddo, N.A., Hoostal, M., Li, X., Wang, T.D., Feehley, T., et al. (2017). Neonatal acquisition of Clostridia species protects against colonization by bacterial pathogens. *Science* **356**, 315–319.
16. Ricklin, D., Reis, E.S., and Lambris, J.D. (2016). Complement in disease: a defence system turning offensive. *Nat. Rev. Nephrol.* **12**, 383–401.
17. Ricklin, D., Hajishengallis, G., Yang, K., and Lambris, J.D. (2010). Complement: a key system for immune surveillance and homeostasis. *Nat. Immunol.* **11**, 785–797.
18. Nesargikar, P.N., Spiller, B., and Chavez, R. (2012). The complement system: history, pathways, cascade and inhibitors. *Eur. J. Microbiol. Immunol. (Bp)* **2**, 103–111.
19. Liszewski, M.K., Java, A., Schramm, E.C., and Atkinson, J.P. (2017). Complement dysregulation and disease: insights from contemporary genetics. *Annu. Rev. Pathol.* **12**, 25–52.
20. Kolev, M., Le Fric, G., and Kemper, C. (2014). Complement—tapping into new sites and effector systems. *Nat. Rev. Immunol.* **14**, 811–820.
21. Heesterbeek, D.A.C., Angelier, M.L., Harrison, R.A., and Rooijackers, S.H.M. (2018). Complement and bacterial infections: from molecular mechanisms to therapeutic applications. *J. Innate Immun.* **10**, 455–464.
22. Cavaillon, J.M., Sansonetti, P., and Goldman, M. (2019). 100th Anniversary of Jules Bordet's Nobel Prize: tribute to a Founding Father of Immunology. *Front. Immunol.* **10**, 2114.
23. Boudry, G., Charton, E., Le Huerou-Luron, I., Ferret-Bernard, S., Le Gall, S., Even, S., and Blat, S. (2021). The relationship between breast milk components and the infant gut microbiota. *Front. Nutr.* **8**, 629740.
24. Korhonen, H., Marnila, P., and Gill, H.S. (2000). Milk immunoglobulins and complement factors. *Br. J. Nutr.* **84 (Suppl 1)**, S75–S80.
25. Zhang, L., Boeren, S., Hageman, J.A., van Hooijdonk, T., Vervoort, J., and Hettinga, K. (2015). Bovine milk proteome in the first 9 days: protein interactions in maturation of the immune and digestive system of the newborn. *PLoS One* **10**, e0116710.
26. Nakajima, S., Baba, A.S., and Tamura, N. (1977). Complement system in human colostrum: presence of nine complement components and factors of alternative pathway in human colostrum. *Int. Arch. Allergy Appl. Immunol.* **54**, 428–433.
27. Rainard, P. (2003). The complement in milk and defense of the bovine mammary gland against infections. *Vet. Res.* **34**, 647–670.
28. Ogundele, M.O. (1999). Complement-mediated bactericidal activity of human milk to a serum-susceptible strain of *E. coli* O111. *J. Appl. Microbiol.* **87**, 689–696.
29. Korhonen, H., Syväoja, E.L., Ahola-Luttilla, H., Sivelä, S., Kopola, S., Husu, J., and Kosunen, T.U. (1995). Bactericidal effect of bovine normal and immune serum, colostrum and milk against *Helicobacter pylori*. *J. Appl. Bacteriol.* **78**, 655–662.
30. Dunkelberger, J.R., and Song, W.C. (2010). Complement and its role in innate and adaptive immune responses. *Cell Res.* **20**, 34–50.
31. Mullineaux-Sanders, C., Sanchez-Garrido, J., Hopkins, E.G.D., Shenoy, A.R., Barry, R., and Frankel, G. (2019). *Citrobacter rodentium*-host-microbiota interactions: immunity, bioenergetics and metabolism. *Nat. Rev. Microbiol.* **17**, 701–715.
32. Collins, J.W., Keeney, K.M., Crepin, V.F., Rathinam, V.A., Fitzgerald, K.A., Finlay, B.B., and Frankel, G. (2014). *Citrobacter rodentium*: infection, inflammation and the microbiota. *Nat. Rev. Microbiol.* **12**, 612–623.
33. Caballero-Flores, G., Pickard, J.M., and Núñez, G. (2021). Regulation of *Citrobacter rodentium* colonization: virulence, immune response and microbiota interactions. *Curr. Opin. Microbiol.* **63**, 142–149.
34. Gros, P., Milder, F.J., and Janssen, B.J. (2008). Complement driven by conformational changes. *Nat. Rev. Immunol.* **8**, 48–58.
35. Ricklin, D., Reis, E.S., Mastellos, D.C., Gros, P., and Lambris, J.D. (2016). Complement component C3 – The “Swiss Army Knife” of innate immunity and host defense. *Immunol. Rev.* **274**, 33–58.
36. Thielens, N.M., Tedesco, F., Bohlson, S.S., Gaboriaud, C., and Tenner, A.J. (2017). C1q: A fresh look upon an old molecule. *Mol. Immunol.* **89**, 73–83.
37. Reid, K.B.M. (2018). Complement Component C1q: historical perspective of a functionally versatile, and structurally unusual, serum protein. *Front. Immunol.* **9**, 764.
38. Kishore, U., Thielens, N.M., and Gaboriaud, C. (2016). Editorial: State-of-the-art research on C1q and the classical complement pathway. *Front. Immunol.* **7**, 398.
39. Bajic, G., Degn, S.E., Thiel, S., and Andersen, G.R. (2015). Complement activation, regulation, and molecular basis for complement-related diseases. *EMBO J.* **34**, 2735–2757.
40. Ogundele, M. (2001). Role and significance of the complement system in mucosal immunity: particular reference to the human breast milk complement. *Immunol. Cell Biol.* **79**, 1–10.
41. Rogier, E.W., Frantz, A.L., Bruno, M.E., Wedlund, L., Cohen, D.A., Stromberg, A.J., and Kaetzel, C.S. (2014). Secretory antibodies in breast milk promote long-term intestinal homeostasis by regulating the gut microbiota and host gene expression. *Proc. Natl. Acad. Sci. USA* **111**, 3074–3079.
42. Rollins, S.A., Zhao, J., Ninomiya, H., and Sims, P.J. (1991). Inhibition of homologous complement by CD59 is mediated by a species-selective recognition conferred through binding to C8 within C5b-8 or C9 within C5b-9. *J. Immunol.* **146**, 2345–2351.
43. Davies, A., Simmons, D.L., Hale, G., Harrison, R.A., Tighe, H., Lachmann, P.J., and Waldmann, H. (1989). CD59, an LY-6-like protein expressed in human lymphoid cells, regulates the action of the complement membrane attack complex on homologous cells. *J. Exp. Med.* **170**, 637–654.
44. Singh, B., Su, Y.C., and Riesbeck, K. (2010). Vitronectin in bacterial pathogenesis: a host protein used in complement escape and cellular invasion. *Mol. Microbiol.* **78**, 545–560.
45. Milis, L., Morris, C.A., Sheehan, M.C., Charlesworth, J.A., and Pussell, B.A. (1993). Vitronectin-mediated inhibition of complement: evidence for different binding sites for C5b-7 and C9. *Clin. Exp. Immunol.* **92**, 114–119.
46. Gaboriaud, C., Ling, W.L., Thielens, N.M., Bally, I., and Rossi, V. (2014). Deciphering the fine details of c1 assembly and activation mechanisms: “mission impossible”? *Front. Immunol.* **5**, 565.

47. Wallis, R., Mitchell, D.A., Schmid, R., Schwaeble, W.J., and Keeble, A.H. (2010). Paths reunited: initiation of the classical and lectin pathways of complement activation. *Immunobiology* 215, 1–11.
48. Kashyap, D.R., Wang, M., Liu, L.H., Boons, G.J., Gupta, D., and Dziarski, R. (2011). Peptidoglycan recognition proteins kill bacteria by activating protein-sensing two-component systems. *Nat. Med.* 17, 676–683.
49. Harriman, G.R., Podack, E.R., Braude, A.I., Corbeil, L.C., Esser, A.F., and Curd, J.G. (1982). Activation of complement by serum-resistant *Neisseria gonorrhoeae*. Assembly of the membrane attack complex without subsequent cell death. *J. Exp. Med.* 156, 1235–1249.
50. Joiner, K.A., Brown, E.J., and Frank, M.M. (1984). Complement and bacteria: chemistry and biology in host defense. *Annu. Rev. Immunol.* 2, 461–491.
51. Tomlinson, S., Taylor, P.W., Morgan, B.P., and Luzio, J.P. (1989). Killing of gram-negative bacteria by complement. Fractionation of cell membranes after complement C5b-9 deposition on to the surface of *Salmonella minnesota* Re595. *Biochem. J.* 263, 505–511.
52. Bloch, E.F., Knight, E.M., Carmon, T., McDonald-Pinkett, S., Carter, J., Boomer, A., Ogunfusika, M., Petersen, M., Famakin, B., Aniagolu, J., et al. (1997). C5b-7 and C5b-8 precursors of the membrane attack complex (C5b-9) are effective killers of *E. coli* J5 during serum incubation. *Immunol. Invest.* 26, 409–419.
53. Murphy, K., Weaver, C., and Janeway, C. (2017). *Janeway's Immunobiology*, Ninth Edition (W.W. Norton & Company).
54. Kitamura, D., Roes, J., Kühn, R., and Rajewsky, K. (1991). A B cell-deficient mouse by targeted disruption of the membrane exon of the immunoglobulin mu chain gene. *Nature* 350, 423–426.
55. Sarkar, A., Yoo, J.Y., Valeria Ozorio Dutra, S., Morgan, K.H., and Groer, M. (2021). The association between early-life gut microbiota and long-term health and diseases. *J. Clin. Med.* 10, 459.
56. Gaufin, T., Tobin, N.H., and Aldrovandi, G.M. (2018). The importance of the microbiome in pediatrics and pediatric infectious diseases. *Curr. Opin. Pediatr.* 30, 117–124.
57. Derrien, M., Alvarez, A.S., and de Vos, W.M. (2019). The gut microbiota in the first decade of life. *Trends Microbiol.* 27, 997–1010.
58. Pannaraj, P.S., Li, F., Cerini, C., Bender, J.M., Yang, S., Rollie, A., Adisetiyo, H., Zabih, S., Lincez, P.J., Bittinger, K., et al. (2017). Association between breast milk bacterial communities and establishment and development of the infant gut microbiome. *JAMA Pediatr.* 171, 647–654.
59. Atyeo, C., and Alter, G. (2021). The multifaceted roles of breast milk antibodies. *Cell* 184, 1486–1499.
60. Adlerberth, I., Lindberg, E., Aberg, N., Hesselmar, B., Saalman, R., Stranegård, I.L., and Wold, A.E. (2006). Reduced enterobacterial and increased staphylococcal colonization of the infantile bowel: an effect of hygienic lifestyle? *Pediatr. Res.* 59, 96–101.
61. Bäckhed, F., Roswall, J., Peng, Y., Feng, Q., Jia, H., Kovatcheva-Datchary, P., Li, Y., Xia, Y., Xie, H., Zhong, H., et al. (2015). Dynamics and stabilization of the human gut microbiome during the first year of life. *Cell Host Microbe* 17, 690–703.
62. Berends, E.T., Dekkers, J.F., Nijland, R., Kuipers, A., Soppe, J.A., van Strijp, J.A., and Rooijackers, S.H. (2013). Distinct localization of the complement C5b-9 complex on Gram-positive bacteria. *Cell. Microbiol.* 15, 1955–1968.
63. Diebold, C.A., Beurskens, F.J., de Jong, R.N., Koning, R.I., Strumane, K., Lindorfer, M.A., Voorhorst, M., Ugurlar, D., Rosati, S., Heck, A.J., et al. (2014). Complement is activated by IgG hexamers assembled at the cell surface. *Science* 343, 1260–1263.
64. Betz, S.J., and Isliker, H. (1981). Antibody-independent interactions between *Escherichia coli* J5 and human complement components. *J. Immunol.* 127, 1748–1754.
65. Clas, F., and Loos, M. (1981). Antibody-independent binding of the first component of complement (C1) and its subcomponent C1q to the S and R forms of *Salmonella Minnesota*. *Infect. Immun.* 31, 1138–1144.
66. Tenner, A.J., Ziccardi, R.J., and Cooper, N.R. (1984). Antibody-independent C1 activation by *E. coli*. *J. Immunol.* 133, 886–891.
67. Albertí, S., Marqués, G., Camprubí, S., Merino, S., Tomás, J.M., Vivanco, F., and Benedí, V.J. (1993). C1q binding and activation of the complement classical pathway by *Klebsiella pneumoniae* outer membrane proteins. *Infect. Immun.* 61, 852–860.
68. Mintz, C.S., Arnold, P.I., Johnson, W., and Schultz, D.R. (1995). Antibody-independent binding of complement component C1q by *Legionella pneumophila*. *Infect. Immun.* 63, 4939–4943.
69. Loos, M., Clas, F., and Fischer, W. (1986). Interaction of purified lipoteichoic acid with the classical complement pathway. *Infect. Immun.* 53, 595–599.
70. Wilkinson, B.J., Kim, Y., and Peterson, P.K. (1981). Factors affecting complement activation by *Staphylococcus aureus* cell walls, their components, and mutants altered in teichoic acid. *Infect. Immun.* 32, 216–224.
71. Danino, T., Prindle, A., Kwong, G.A., Skalak, M., Li, H., Allen, K., Hasty, J., and Bhatia, S.N. (2015). Programmable probiotics for detection of cancer in urine. *Sci. Transl. Med.* 7, 289ra84.
72. Archer, N.K., Wang, Y., Ortines, R.V., Liu, H., Nolan, S.J., Liu, Q., Alphonse, M.P., Dikeman, D.A., Mazhar, M., Miller, R.J., et al. (2020). Pre-clinical models and methodologies for monitoring *Staphylococcus aureus* infections using noninvasive optical imaging. *Methods Mol. Biol.* 2069, 197–228.
73. Bolger, A.M., Lohse, M., and Usadel, B. (2014). Trimmomatic: a flexible trimmer for Illumina sequence data. *Bioinformatics* 30, 2114–2120.
74. Bolyen, E., Rideout, J.R., Dillon, M.R., Bokulich, N.A., Abnet, C.C., Al-Ghalith, G.A., Alexander, H., Alm, E.J., Arumugam, M., Asnicar, F., et al. (2019). Reproducible, interactive, scalable and extensible microbiome data science using QIIME 2. *Nat. Biotechnol.* 37, 852–857.
75. Xia, X., Liu, Y., Hodgson, A., Xu, D., Guo, W., Yu, H., She, W., Zhou, C., Lan, L., Fu, K., et al. (2019). EspF is crucial for *Citrobacter rodentium*-induced tight junction disruption and lethality in immunocompromised animals. *PLoS Pathog.* 15, e1007898.
76. Liu, Y., Fu, K., Wier, E.M., Lei, Y., Hodgson, A., Xu, D., Xia, X., Zheng, D., Ding, H., Sears, C.L., et al. (2022). Bacterial genotoxin accelerates transient infection-driven murine colon tumorigenesis. *Cancer Discov.* 12, 236–249.
77. Subramanian, S., Huq, S., Yatsunenkov, T., Haque, R., Mahfuz, M., Alam, M.A., Benzera, A., DeStefano, J., Meier, M.F., Muegge, B.D., et al. (2014). Persistent gut microbiota immaturity in malnourished Bangladeshi children. *Nature* 510, 417–421.
78. Blanton, L.V., Charbonneau, M.R., Salih, T., Barratt, M.J., Venkatesh, S., Ilkaveya, O., Subramanian, S., Manary, M.J., Trehan, I., Jorgensen, J.M., et al. (2016). Gut bacteria that prevent growth impairments transmitted by microbiota from malnourished children. *Science* 351, 830.
79. Caporaso, J.G., Lauber, C.L., Walters, W.A., Berg-Lyons, D., Huntley, J., Fierer, N., Owens, S.M., Betley, J., Fraser, L., Bauer, M., et al. (2012). Ultra-high-throughput microbial community analysis on the Illumina HiSeq and MiSeq platforms. *ISME J.* 6, 1621–1624.
80. Amir, A., McDonald, D., Navas-Molina, J.A., Kopylova, E., Morton, J.T., Zech Xu, Z., Kightley, E.P., Thompson, L.R., Hyde, E.R., Gonzalez, A., et al. (2017). Deblur rapidly resolves single-nucleotide community sequence patterns. *mSystems* 2, e00191-16.
81. Katoh, K., Misawa, K., Kuma, K., and Miyata, T. (2002). MAFFT: a novel method for rapid multiple sequence alignment based on fast Fourier transform. *Nucleic Acids Res.* 30, 3059–3066.
82. Price, M.N., Dehal, P.S., and Arkin, A.P. (2010). FastTree 2—approximately maximum-likelihood trees for large alignments. *PLoS One* 5, e9490.
83. Bokulich, N.A., Kaehler, B.D., Rideout, J.R., Dillon, M., Bolyen, E., Knight, R., Huttley, G.A., and Gregory Caporaso, J. (2018). Optimizing taxonomic classification of marker-gene amplicon sequences with QIIME 2's q2-feature-classifier plugin. *Microbiome* 6, 90.

84. McDonald, D., Price, M.N., Goodrich, J., Nawrocki, E.P., DeSantis, T.Z., Probst, A., Andersen, G.L., Knight, R., and Hugenholtz, P. (2012). An improved Greengenes taxonomy with explicit ranks for ecological and evolutionary analyses of bacteria and archaea. *ISME J.* 6, 610–618.
85. Lozupone, C.A., Hamady, M., Kelley, S.T., and Knight, R. (2007). Quantitative and qualitative beta diversity measures lead to different insights into factors that structure microbial communities. *Appl. Environ. Microbiol.* 73, 1576–1585.
86. Lozupone, C., and Knight, R. (2005). UniFrac: a new phylogenetic method for comparing microbial communities. *Appl. Environ. Microbiol.* 71, 8228–8235.
87. Anderson, M.J. (2017). Permutational multivariate analysis of variance (PERMANOVA). In *Wiley STATSOFT: Statistics Reference Online* (Wiley), pp. 1–15.
88. Mandal, S., Van Treuren, W., White, R.A., Eggesbø, M., Knight, R., and Peddada, S.D. (2015). Analysis of composition of microbiomes: a novel method for studying microbial composition. *Microb. Ecol. Health Dis.* 26, 27663.
89. Willingham, K., McNulty, E., Anderson, K., Hayes-Klug, J., Nalls, A., and Mathiason, C. (2014). Milk collection methods for mice and Reeves' muntjac deer. *J. Vis. Exp.*, 51007.
90. Power, M.L., Schulkin, J., Drought, H., Milligan, L.A., Murtough, K.L., and Bernstein, R.M. (2017). Patterns of milk macronutrients and bioactive molecules across lactation in a western lowland gorilla (*Gorilla gorilla*) and a Sumatran orangutan (*Pongo abelii*). *Am. J. Primatol.* 79, 1–11.
91. Ge, S.X., Jung, D., and Yao, R. (2020). ShinyGO: a graphical gene-set enrichment tool for animals and plants. *Bioinformatics* 36, 2628–2629.
92. Fu, K., Sun, X., Wier, E.M., Hodgson, A., Liu, Y., Sears, C.L., and Wan, F. (2016). Sam68/KHDRBS1 is critical for colon tumorigenesis by regulating genotoxic stress-induced NF- κ B activation. *eLife* 5, e15018.
93. Bankevich, A., Nurk, S., Antipov, D., Gurevich, A.A., Dvorkin, M., Kulikov, A.S., Lesin, V.M., Nikolenko, S.I., Pham, S., Pribelski, A.D., et al. (2012). SPAdes: a new genome assembly algorithm and its applications to single-cell sequencing. *J. Comput. Biol.* 19, 455–477.
94. Yang, J., Wang, J., Yao, Z.J., Jin, Q., Shen, Y., and Chen, R. (2003). GenomeComp: a visualization tool for microbial genome comparison. *J. Microbiol. Methods* 54, 423–426.
95. Grant, J.R., Enns, E., Marinier, E., Mandal, A., Herman, E.K., Chen, C.Y., Graham, M., Van Domselaar, G., and Stothard, P. (2023). Proksee: in-depth characterization and visualization of bacterial genomes. *Nucleic Acids Res.* 51, W484–W492.
96. Scarff, C.A., Fuller, M.J.G., Thompson, R.F., and Iadanza, M.G. (2018). Variations on negative stain electron microscopy methods: tools for tackling challenging systems. *J. Vis. Exp.*, 57199.

STAR★METHODS

KEY RESOURCES TABLE

REAGENT or RESOURCE	SOURCE	IDENTIFIER
Antibodies		
Goat anti-human C1s	Complement Technology	Cat# A204
Rabbit Anti-Human C5b-9	Bioss Antibodies	Cat# bs-2673R; RRID:AB_10855202
HRP-conjugated Goat Anti-Mouse IgG	SouthernBiotech	Cat# 1030-05; RRID:AB_2619742
HRP-conjugated Goat Anti-Mouse IgM	SouthernBiotech	Cat# 1021-05; RRID:AB_2794240
HRP-conjugated Goat Anti-Human IgG	SouthernBiotech	Cat# 2040-05; RRID:AB_2795644
HRP-conjugated Goat Anti-Human IgM	SouthernBiotech	Cat# 2020-05; RRID:AB_2795603
Alexa Fluor 488 conjugated Goat Anti-Rabbit IgG (H+L)	Thermo Fisher Scientific	Cat# A-11034; RRID:AB_2576217
Biotin anti-human IgG	BioLegend	Cat# 410718; RRID:AB_2721499
Biotin anti-human IgM	BioLegend	Cat# 314504; RRID:AB_493007
Bacterial and Virus Strains		
<i>Citrobacter rodentium</i> (DBS100 strain)	ATCC	ATCC# 51459
<i>Escherichia coli</i> (Nissle 1917 strain)	Danino et al. ⁷¹	N/A
<i>Staphylococcus aureus</i> (SH1000 strain)	Archer et al. ⁷²	N/A
<i>Staphylococcus lentus</i> (B3 strain)	This paper	N/A
Biological Samples		
Human breast milk	Mother's Milk Bank	N/A
Chemicals, Peptides, and Recombinant Proteins		
Hoechst 33342	Thermo Fisher Scientific	Cat# H1399
FM5-95	Thermo Fisher Scientific	Cat# T23360
DAPI (4',6-Diamidino-2-phenylindole dihydrochloride)	Sigma-Aldrich	Cat# D8417
DTT (Dithiothreitol)	Sigma-Aldrich	Cat# D9779
FITC-dextran	Sigma-Aldrich	Cat# FD4
Oxytocin	Sigma-Aldrich	Cat# O4375
Ponceau S solution	Sigma-Aldrich	Cat# P7170
NuPAGE LDS Sample Buffer	Thermo Fisher Scientific	Cat# NP0007
DIBAC ₄ (3) [Bis-(1,3-Dibutylbarbituric Acid) Trimethine Oxonol]	Cayman Chemical	Cat# 33924
CCCP (Carbonyl cyanide <i>m</i> -chlorophenyl hydrazone)	Cayman Chemical	Cat# 25458
Recombinant Human CD59 Protein	Sino Biological	Cat# 12474-H08H
Uranyl Acetate	Electron Microscopy Sciences	Cat# 22400
2.5% Glutaraldehyde in 0.1M Sodium Cacodylate Buffer	Electron Microscopy Sciences	Cat# 16537-15
Neomycin sulfate	Santa Cruz Biotechnology	Cat# sc-3573
Vancomycin Hydrochloride	Santa Cruz Biotechnology	Cat# sc-204938A
Cefoxitin	Sagent Pharmaceuticals	NDC 25021-109-10
Sterilizable Fenbendazole Diet	Envigo	Cat# TD.01432
Phenol:Chloroform:Isoamyl Alcohol (25:24:1)	Sigma-Aldrich	Cat# P2069
Tryptic Soy Broth	Millipore	Cat# 22092
MacConkey agar	Criterion	Cat# C6131
Lennox L Broth	Research Products International	Cat# L24066
Lennox L Agar	Research Products International	Cat# L24030
Bovine Serum Albumin	Research Products International	Cat# A30075

(Continued on next page)

Continued

REAGENT or RESOURCE	SOURCE	IDENTIFIER
Trypsin Protease	Thermo Fisher Scientific	Cat# 90057
Critical Commercial Assays		
NucleoSpin Tissue Kit	Macherey-Nagel	Cat# 740952.50
Mouse Immunoglobulin Isotyping ELISA kit	Thermo Fisher Scientific	Cat# 88-50630-88
BCA Protein Assay Kit	Thermo Fisher Scientific	Cat# 23225
TruSeq Nano DNA Library Prep Kit	Illumina	Cat# 20015965
GeneJET Gel Extraction Kit	Thermo Fisher Scientific	Cat# K0691
Ion Plus Fragment Library Kit	Thermo Fisher Scientific	Cat# 4471252
Streptavidin Magnetic Beads	Thermo Fisher Scientific	Cat# 88816
BeadBug prefilled tubes with 0.1mm Silica glass beads	Sigma-Aldrich	Cat# Z763721
Milk Bacterial DNA isolation Kit	Norgen Biotek	Cat# 21550
PureLink Microbiome DNA Purification Kit	Thermo Fisher Scientific	Cat# A29789
Phusion High-Fidelity PCR Master Mix	New England Biolabs	Cat# M0531S
Deposited Data		
16S rRNA gene profiling data	NCBI	NCBI accession: BioProject PRJNA796457
<i>S. lentus</i> B3 whole genome sequencing data	NCBI	NCBI accession: BioProject PRJNA796456
<i>S. lentus</i> H29	GenBank	GenBank accessions: CP059679
<i>S. lentus</i> NCTC12102	GenBank	GenBank accessions: UHDR01000002
<i>S. aureus</i> MW2	NCBI	NCBI Reference Sequence: NC_003923
<i>S. epidermidis</i> RP62A	NCBI	NCBI Reference Sequence: NC_002976
<i>S. haemolyticus</i> JCSC1435	NCBI	NCBI Reference Sequence: NC_007168
<i>S. saprophyticus</i> ATCC15305	NCBI	NCBI Reference Sequence: NC_007350
SwissProt 2020 <i>Mus musculus</i> database	UniProtKB	https://www.uniprot.org
Experimental Models: Organisms/Strains		
Mouse: C57Bl/6J mice	Jackson Laboratory	Strain# 000664; RRID:IMSR_JAX:000664
Mouse: <i>C1qc</i> ^{-/-} : C57BL/6NJ- <i>C1qc</i> ^{em1(IMPC)/J}	Jackson Laboratory	Strain# 029409; RRID:IMSR_JAX:029409
Mouse: <i>C3</i> ^{-/-} : B6.129S4- <i>C3</i> ^{tm1Crr/J}	Jackson Laboratory	Strain# 029661; RRID:IMSR_JAX:029661
Mouse: <i>μMT</i> ^{-/-} : B6.129S2- <i>Ighm</i> ^{tm1Cgn/J}	Jackson Laboratory	Strain# 002288; RRID:IMSR_JAX:002288
Software and Algorithms		
GraphPad Prism 9.4.0	GraphPad	https://www.graphpad.com/
FlowJo 10.9.0	BD	https://www.flowjo.com/solutions/flowjo
Adobe Illustrator	Adobe	https://www.adobe.com/products/illustrator.html
Adobe Photoshop	Adobe	https://www.adobe.com/products/photoshop.html
Proteome Discoverer v2.4	Thermo Fisher Scientific	https://www.thermofisher.com/us/en/home/industrial/mass-spectrometry/liquid-chromatography-mass-spectrometry-lc-ms/lc-ms-software/multi-omics-data-analysis/teome-discoverer-software.html
Mascot v.2.6.2	Matrix Science	https://www.matrixscience.com/mascot_support_v2_6.html
Scaffold 4	Proteome Software	https://www.proteomesoftware.com
ShinyGO v0.741	South Dakota State University	http://bioinformatics.sdstate.edu/go/
FV31S-SW_V2.1	Olympus	https://www.olympus-lifescience.com/en/downloads/detail-iframe/?0[downloads][id]=847252002
Fiji	Image J	https://imagej.net/software/fiji/downloads
Trimmomatic software V0.32	Bolger et al. ⁷³	http://www.usadellab.org/cms/index.php?page=trimmomatic
QIIME 2	QIIME 2 development team ⁷⁴	https://library.qiime2.org/about/

RESOURCE AVAILABILITY

Lead contact

Further information and requests for resources and reagents should be directed to and will be fulfilled by the lead contact, Fengyi Wan (fwan1@jhu.edu).

Materials availability

All unique/stable reagents generated in this study are available from the [lead contact](#) with a completed materials transfer agreement.

Data and code availability

- 16S rRNA gene profiling data and *S. lentus* B3 whole genome sequencing data have been deposited in the National Center for Biotechnology Information (NCBI) database and are publicly available as of the date of publication. This paper also analyzes sequencing data of bacteria *S. lentus* (H29 strain), *S. lentus* (NCTC12102 strain), *S. aureus* (MW2 strain), *S. epidermidis* (RP62A strain), *S. haemolyticus* (JCSC1435 strain), and *S. saprophyticus* (ATCC15305 strain), as well as *Mus musculus* database, all of which are existing and publicly available. These accession numbers for the datasets are listed in the [key resources table](#).
- This paper does not report original code.
- Any additional information required to reanalyze the data reported in this paper is available from the [lead contact](#) upon request.

EXPERIMENTAL MODEL AND STUDY PARTICIPANT DETAILS

Animals

Wild-type C57Bl/6J mice (stock no. 000664) and *C1qc*^{-/-} mice (stock no. 029409) were purchased from The Jackson Laboratory (Bar Harbor, ME). *C3*^{-/-} and μ MT^{-/-} mice were kindly shared by S. Lajoie and M. Mugnier (Johns Hopkins University), respectively. Wild-type C57Bl/6J and *C1qc*^{-/-} mice (8-20 weeks old) were crossed to generate *C1qc*^{+/-} pups. *C1qc*^{-/-} and μ MT^{-/-} mice (8-20 weeks old) were bred to generate F₁ *C1qc*^{+/-} μ MT^{+/-} progeny; and F₁ *C1qc*^{+/-} μ MT^{+/-} mice (8-20 weeks old) were used to generate F₂ *C1qc*^{-/-} μ MT^{-/-} progeny. All mice were fed sterilized food and water *ad libitum* and maintained in a specific pathogen free (SPF) mouse facility. C57Bl/6J and *C1qc*^{-/-} mice were rederived as germ free (GF) using a standard protocol and maintained in the GF mouse facilities at Johns Hopkins University in flexible-film isolators. Sterility was verified at regular intervals using aerobic cultures, anaerobic cultures, and PCR. Mouse genotyping was conducted per the Jackson Laboratory genotyping protocol for the corresponding stock numbers. Except that breast milk samples were collected from female mice during lactation periods, male and female mice (age ranging from weanling [21-day-old] to adulthood [6-8-week-old] as indicated in [method details](#)) were used for all experiments. Littermates of the same sex were randomly assigned to different experimental groups. All animal experiments were performed according to protocols approved by the Johns Hopkins University's Animal Care and Use Committee and in direct accordance with the NIH guidelines for housing and care of laboratory animals.

Microbe strains

Citrobacter rodentium (CR, DBS100 strain, ATCC No. 51459) was purchased from the American Type Culture Collection (ATCC, Manassas, VA). *Escherichia coli* (Nissle 1917 strain) was kindly shared by T. Danino (Columbia University).⁷¹ *Staphylococcus lentus* (B3 strain) was isolated in this study. All of them were grown from single colonies on Luria-Bertani (LB) plates in LB broth at 37°C overnight with shaking. *S. aureus* (SH1000 strain) was kindly shared by N. Archer (Johns Hopkins University)⁷² and cultured in Tryptic Soy Broth (TSB) with chloramphenicol.

Human breast milk samples

The randomly selected and de-identified human breast milk samples from healthy donors were kindly provided by Mother's Milk Bank in San Jose (www.mothersmilk.org). The donors are healthy lactating women from variant racial background and approved using a specialized clinical review typically including an oral or written interview, screening for general health and medication use, and serological testing.

METHOD DETAILS

Cross-fostering experiments

The breeding pairs (one male and one female) of wild-type C57Bl/6J, *C1qc*^{-/-}, and *C3*^{-/-} were synchronized to generate pups born on the same day for subsequent cross-fostering with the dams switched at the day of birth. After 21 days of cross-fostering, pups were separated and used for CR infection experiments.

Reconstitution of GF mice with SPF commensal microbiota

Wild-type and *C1qc*^{-/-} donor mice (21 days old) maintained in SPF mouse facility were sacrificed in a BACTRON anaerobic chamber (Sheldon, Cornelius, OR). The cecal and colonic contents were collected and diluted into 5 mL sterile PBS, and the suspension was passed through 40 μm nylon filter to remove particulate matter. Fresh slurries were orally gavaged (200 μL per mouse) into GF *C1qc*^{-/-} recipients (17 days old). Four days later, the transferred GF *C1qc*^{-/-} mice were challenged with an oral infection with CR or vehicle control.

Bacterial infection in mice

CR infection in mice was conducted as described previously.⁷⁵ In brief, pups (males and females), separated from their dams on 21 days postnatal (P21), were inoculated by oral gavage with 200 μL of PBS containing 2×10^9 colony-forming units (CFU) of CR or PBS vehicle control. Adult mice (6–8 weeks old) were infected as described above; the body weight, clinical scores, and survival of infected mice were monitored daily. For fecal CR burden analysis, stool was collected from live animals at various time periods post-inoculation. The stool and tissue were homogenized and diluted in sterile PBS at 10 mL per gram of stool or tissue, plated on MacConkey agar plates, and CFUs were enumerated at the following day.

Histology and immunofluorescence

Histology and immunofluorescence staining of colon tissue sections were performed as previously described.⁷⁶ In brief, after euthanizing mice, the colon was removed under aseptic conditions, washed once with ice-cold PBS, fixed in 10% buffered formalin for 24 hours, and processed for paraffin embedding. Sections (5 μm) were cut and processed for Hematoxylin and Eosin (H&E) staining. Histopathology scores were determined in a blinded fashion using the previously described criteria.⁷⁵

FITC-dextran assays

FITC-dextran assays for intestinal permeability were performed as previously described.⁷⁵ In brief, mice were administered with 150 μL of 80 mg/mL FITC-dextran (4,000 Da, FD4, Sigma) in PBS by oral gavage. After 4 hours, mice were anaesthetized, and blood was collected by cardiac puncture. After centrifugation at $1,000 \times g$ at 4°C for 15 minutes and the levels of FITC-dextran in the plasma was measured using a BioTek Synergy HT microplate reader (BioTek, Winooski, VT) at excitation 485 nm and emission 528 nm.

Flow cytometry and confocal microscopy

S. lentus (B3 strain), incubated for 2 hours with indicated human whey, were washed twice with PBS-1% BSA and incubated with 2 μg/mL rabbit anti-C5b-9 (bs-2673R, Bioss) in 100 μL PBS-1% BSA at 4°C. After 1 hour incubation, bacteria was washed twice with PBS-1% BSA, followed by incubation with 2 μg/mL Alexa Fluor488 conjugated goat anti-rabbit IgG in 100 μL PBS-1% BSA (Thermo Fisher Scientific) for 45 minutes at 4°C. For flow cytometry, bacteria were washed and resuspended with PBS, then analyzed on Cytex NL-3000 flow cytometer (Cytex Biosciences, Fremont, CA). Data were analyzed using the FlowJo software (version 10, BD Life Sciences). For confocal microscopy, *S. lentus* (B3 strain) was incubated with indicated human whey and stained with anti-C5b-9 and Alexa Fluor 488 conjugated antibodies as described above. Following counterstaining of bacterial DNA and membrane with Hoechst 33342 (1 μg/mL) and FM5-95 (5 μg/mL), respectively, bacterial samples were mounted with coverslip, sealed, and imaged immediately with Olympus FV3000RS confocal microscope equipped with UPLSAPO 100× SI OIL objective (Olympus, Tokyo, Japan).

Microbiota composition

Total genomic DNA from the cecal and colonic contents, collected from indicated pups (21 days old), was extracted as previously described.^{77,78} Briefly, cecal and colonic contents were transferred to BeadBug™ prefilled microtubes (2 mL) with 500 μL of 0.1 mm acid washed Silica glass beads (Z763721, Sigma-Aldrich), suspended with 500 μL of extraction buffer (200 mM Tris-HCl, pH 8.0, 200 mM NaCl, 20 mM EDTA), 210 μL of 20% SDS, 500 μL of phenol:chloroform:isoamyl alcohol solution (25:24:1, v/v, Sigma-Aldrich). Samples were disrupted on a VWR Bead Mill Homogenizer (VWR) at maximum speed for 10 minutes to ensure uniform and efficient cell lysis, followed by DNA extraction with phenol:chloroform:isoamyl alcohol solution and DNA precipitation with iso-propanol (Sigma-Aldrich), respectively. Bacterial genomic DNA from stomach, small intestinal contents, and breast milk contents was extracted using PureLink Microbiome DNA Purification Kit (Thermo Fisher Scientific) and Milk Bacterial DNA isolation Kit (Norgen Biotek), respectively. DNA concentration and purity were monitored on 1% agarose gels, followed by normalization to the same concentration (1 ng/μL). The V4 region of 16S rRNA gene were amplified using Phusion® High-Fidelity PCR Master Mix (New England Biolabs), with the published primer pair of 515F (5'-GTGCCAGCMGCCGCGGTAA-3') and 806R (5'-GGAC TACHVGGGTWCTAAT-3')⁷⁹ with the barcode. PCR products were separated by agarose gel electrophoresis for detection, mixed in equidensity ratios, and purified with GeneJET™ Gel Extraction Kit (Thermo Fisher Scientific). Sequencing libraries were generated using Ion Plus Fragment Library Kit (Thermo Fisher Scientific) following manufacturer's recommendations. The library quality was assessed on the Qubit@ 2.0 Fluorometer (Thermo Fisher Scientific), followed by sequencing on an Ion S5™ XL platform (400-bp single read) or a NovaSeq 6000 platform (250-bp paired end reads) at Novogene (Sacramento, CA). A mean sequence depth of 155,620 tags per sample was obtained. Reads were assigned to samples based on their unique barcodes and quality trimmed using the Trimmomatic software V0.32.⁷³ Microbiome bioinformatics were performed with the QIIME 2 2023.5.⁷⁴ Raw sequence data were

demultiplexed and quality filtered using the q2-demux plugin followed by denoising with Deblur⁸⁰ (via q2-deblur). All amplicon sequence variants (ASVs) were aligned with MAFFT⁸¹ (via q2-alignment) and used to construct a phylogeny with FastTree2⁸² (via q2-phylogeny). Taxonomy was assigned to ASVs using the q2-feature-classifier⁸³ classify-sklearn naïve Bayes taxonomy classifier against the Greengenes 13_8 99% operational taxonomic units (OTUs) reference sequences.⁸⁴ Alpha diversity metrics (observed features, Chao1 index, Shannon index, and Simpson index) and beta diversity metrics (weighted UniFrac⁸⁵ and unweighted UniFrac⁸⁶) were estimated using q2-diversity after samples were rarefied. All these indices were visualized by R scripts V4.3.0 and GraphPad Prism V7.04 (GraphPad Software, Boston, MA). To further evaluate the differences in species complexity of samples from each group (beta diversity), the non-metric multidimensional scaling (NMDS) clustering was conducted by QIIME2 software⁷⁴ with weighted UniFrac distance. A permutational multivariate anova (PERMANOVA) test⁸⁷ was performed to determine the statistical significance for each beta group of NMDS ordination. Significance testing of differences in relative abundance at different taxonomic levels was performed using ANCOM.⁸⁸

Collection of breast milk whey

Manually express milk from the teat of mice were collected as described previously.⁸⁹ Briefly, the dam was separated from the litter (5-15 days) for approximately 2 hours prior to the collection of milk. The dam was injected intraperitoneally with 2 IU/kg of oxytocin. After 5-10 minutes to allow the oxytocin to stimulate milk production, dams were anesthetized, and the mammary tissue was gently massaged until a visible bead of milk formed at the base of the teat. The collected mouse breast milk samples and human breast milk samples (obtained from Mother's Milk Bank) were centrifuged 16,000 × *g* at 4°C for 15 minutes, and the whey phase was collected and stored at -80°C. For complement inactivation, mouse and human whey samples were heated in a water-bath at 56°C for 30 minutes. Mouse whey protein concentration was determined using the BCA Protein Assay Kit (Thermo Fisher Scientific). Dry matter, water content, crude fat, total sugar, crude protein, and gross energy in mouse milk were analyzed as previously described.⁹⁰

Mass spectrometry and protein functional annotation

Mass spectrometry was conducted by the Mass Spectrometry and Proteomics Core Facility at The Johns Hopkins University School of Medicine. In brief, mouse whey proteins were digested with trypsin (Pierce, Dallas, TX) at 1:50 enzyme to protein ratio overnight at 37°C. Tryptic peptides were analyzed by reverse-phase chromatography tandem mass spectrometry on an EasyLC1100 UPLC interfaced with a Orbitrap-Fusion Lumos mass spectrometer (Thermo Fisher Scientific). Fragmentation spectra were processed by Proteome Discoverer v2.4 (PD2.4, Thermo Fisher Scientific) and searched with Mascot v.2.6.2 (Matrix Science, London, UK) against the SwissProt 2020 *Mus musculus* database. Peptide identifications from the Mascot searches were processed and imported into Scaffold (Proteome Software Inc.), validated by Protein Prophet to filter at a 95% confidence on peptides and proteins. The list of whey proteins was subjected to ontology enrichment analysis using the ShinyGO (v0.741) tool,⁹¹ with the species Mouse and KEGG (Kyoto Encyclopedia of Genes and Genomes) pathways selected.

Immunoblot

Mouse whey proteins were mixed with NuPAGE LDS Sample Buffer (Invitrogen, Waltham, MA) and heated at 95°C for 10 minutes, followed by SDS-PAGE under reducing and denaturing conditions. The separated proteins were electro-transferred onto nitrocellulose membranes (Santa Cruz Biotechnology, Dallas, TX) and stained with Ponceau S solution to visualize the transferred material. The membrane was de-stained and immunoblotted with specific antibodies and the Super Signaling system (Thermo Scientific) was used to detect antibody binding according to manufacturer's instructions. The immunoblots were imaged using a FluorChem E System (Protein Simple, Santa Clara, CA), as previously described.⁹²

Breast milk bactericidal assays

Bactericidal activity of mouse breast milk on commensal bacteria (CB) was determined on LB agar plates. Briefly, cecal and colonic contents isolated from P21 pups were suspended in sterile PBS and 20 μL of the suspension was spotted on LB agar plates, and cultured at 25°C. After 30 minutes, 5 μL of mouse whey or PBS vehicle control was layered on the top of the bacteria. The LB agar plates were incubated at 37°C for 16 hours. The milk antimicrobial activity was detected by measuring the colony growth in the whey-covered area. Bactericidal activities of human and mouse milk on the isolated *S. lentus* B3 were examined on LB agar plates and LB medium culture. For LB agar plate assays, 20 μL of 1 × 10⁵ CFU/ml *S. lentus* B3 solution, diluted from an overnight culture with sterile LB medium, was spotted on LB agar and cultured at room temperature. After 30 minutes, 5 μL of whey or PBS vehicle control was added to the center of bacterial culture, and the LB agar plates were incubated and imaged as described above. For LB medium culture assays, 1 × 10⁴ CFU/ml *S. lentus* B3, *S. aureus* SH1000, or *E. coli* N1917 in LB medium, supplemented with 2.5% (v/v) mouse whey, 40% (v/v) human whey, or PBS vehicle control was cultured at 37°C with shaking at 150 rpm. After 16 hours, bacterial concentrations were determined by serial dilutions and plating on LB agar plates. CFUs were enumerated after overnight culture and normalized to the culture volume. For time kill-kinetics assays in LB medium, 1 × 10⁴ CFU/mL *S. lentus* B3, was incubated with 40% (v/v) human whey or PBS vehicle control at 37°C with shaking at 150 rpm. At indicated time points, 100 μL of bacterial culture was plated on LB agar dishes and cultured at 37°C overnight, followed by plate imaging.

Whole genome sequencing, genome assembly, and comparative analysis

Genomic DNA was extracted from overnight culture of *S. lentus* B3 using NucleoSpin Tissue Kit (Macherey-Nagel, Bethlehem, PA) following manufacturer's instructions. DNA concentration and purity were monitored on 1% agarose gels, followed by normalization to the same concentration (1 ng/ μ L). Sequencing libraries were generated using TruSeq Nano DNA Library Prep Kit (Illumina Inc., San Diego, CA) following manufacturer's recommendations. The library quality was assessed on an Agilent TapeStation 4200, followed by sequencing on a NovaSeq6000 S4 platform and 150-bp paired end (PE) reads were generated at Psomagen (Rockville, MD). The quality control of raw sequencing data, 30,126,990 total reads and 4.549 Gb, was conducted using the Trimmomatic v0.36 with settings to trim low-quality bases ($Q < 15$) from both ends of each read. Valid reads were then fed to the *de novo* genome assembler SPAdes v3.9.0 to reconstruct the draft genome of *S. lentus* B3 with default parameters.⁹³ The complete genomes of the *S. lentus* strains H29 and NCTC12102 (GenBank accessions: CP059679 and UHDR01000002) were used to assemble and order contigs to build the *S. lentus* B3 genome. The GenomeComp v1.2⁹⁴ was used for linear comparison of the aforementioned three *S. lentus* genomes, whereas the Proksee⁹⁵ was employed for circular genomic comparison between *S. lentus* B3 and other representative *Staphylococcus* genomes, including *S. lentus* (H29 and NCTC12102), *S. aureus* MW2 (NC_003923), *S. epidermidis* RP62A (NC_002976), *S. haemolyticus* JCSC1435 (NC_007168) and *S. saprophyticus* ATCC15305 (NC_007350).

Enzyme-linked immunosorbent assays

Immunoglobulins in the milk from the dams were measured using a Mouse Immunoglobulin Isotyping ELISA kit (Thermo Fisher Scientific) following manufacturer's instructions. Results were read at a BioTek Synergy HT microplate reader (BioTek) at optical density 450 nm.

Maternal antibiotics treatment

For maternal antibiotics treatment, dams were fed sterile drinking water containing Neomycin (1 mg/mL), Vancomycin (500 μ g/mL), or Cefoxitin (500 μ g/mL), starting from day 7 after giving birth. For Fenbendazole treatment, dams were administered with Sterilizable Fenbendazole Diet (150 ppm, Envigo, Indianapolis, IN) during lactation period. All antibiotic administration was halted on day 19 after birth. Following removal of maternal antibiotics treatment for 48 hours, pups were inoculated with CR by oral gavage.

Membrane depolarization

Fluorescent probe *Bis*-(1,3-Dibutylbarbituric Acid) Trimethine Oxonol [DiBAC₄(3), Cayman Chemical, Ann Arbor, MI] was used to assess membrane depolarization, as previously described.⁴⁸ In brief, *S. lentus* B3 was incubated with whey or PBS control, in the presence or absence of CD59 (200 μ g/mL) or Vitronectin (100 μ g/mL), at 37 °C with 150 rpm shaking. At indicated time periods, bacteria were washed with PBS and stained with 500 μ L of 1 μ g/mL DiBAC₄(3). The protonophore carbonyl cyanide *m*-chlorophenyl hydrazine (CCCP, Cayman Chemical) was included in bacteria suspensions at a final concentration of 10 μ M for 30 minutes for a positive control. Bacterial fluorescence was measured on Cytex NL-3000 flow cytometer (Cytex Biosciences), and data were analyzed using the FlowJo software (BD Life Sciences).

Immunoglobulin depletion in human milk whey

Human whey samples were mock treated or incubated with biotin-conjugated antibodies specific for human IgG and IgM (BioLegend) together with Streptavidin magnetic beads (Thermo Scientific), followed by magnetic column separation. The complete IgG/IgM depletion in human milk whey samples was validated by SDS-PAGE separation and immunoblot, prior to the usage in the indicated assays.

Transmission electron microscopy

S. lentus B3 derived from a log-phase culture was incubated with mouse or human breast-milk-derived whey from the indicated dams for 2 hours, followed by fixation with 2.5% glutaraldehyde in 0.1 M sodium cacodylate buffer for 30 minutes. The cells were washed, suspended with DPBS, and subjected to negative staining, as previously described.⁹⁶ Briefly, 10 μ L of cell suspension was placed onto copper EM grids and stained with 1% uranyl acetate for 1 minute. Following three washes with distilled water, the grids were dried on filter paper for at least 30 minutes and mounted on a Hitachi H7600 Transmission Electron Microscope (Chiyoda, Japan). Specimens were illuminated with a focused beam of electrons in a vacuum chamber at 80 KV electron energy.

QUANTIFICATION AND STATISTICAL ANALYSIS

Statistical analysis was performed using GraphPad Prism version 9.0.1 (GraphPad Software). Standard errors of means (s.e.m.) were plotted in graphs. Statistical significance was determined by Student's *t*-test, one-way ANOVA with Bonferroni post-hoc test, or log-rank (Mantel-Cox) test (survival curves). Significant differences were considered: ns, non-significant difference; * at $p < 0.05$; ** at $p < 0.01$; *** at $p < 0.001$; and **** at $p < 0.0001$.

Supplemental figures

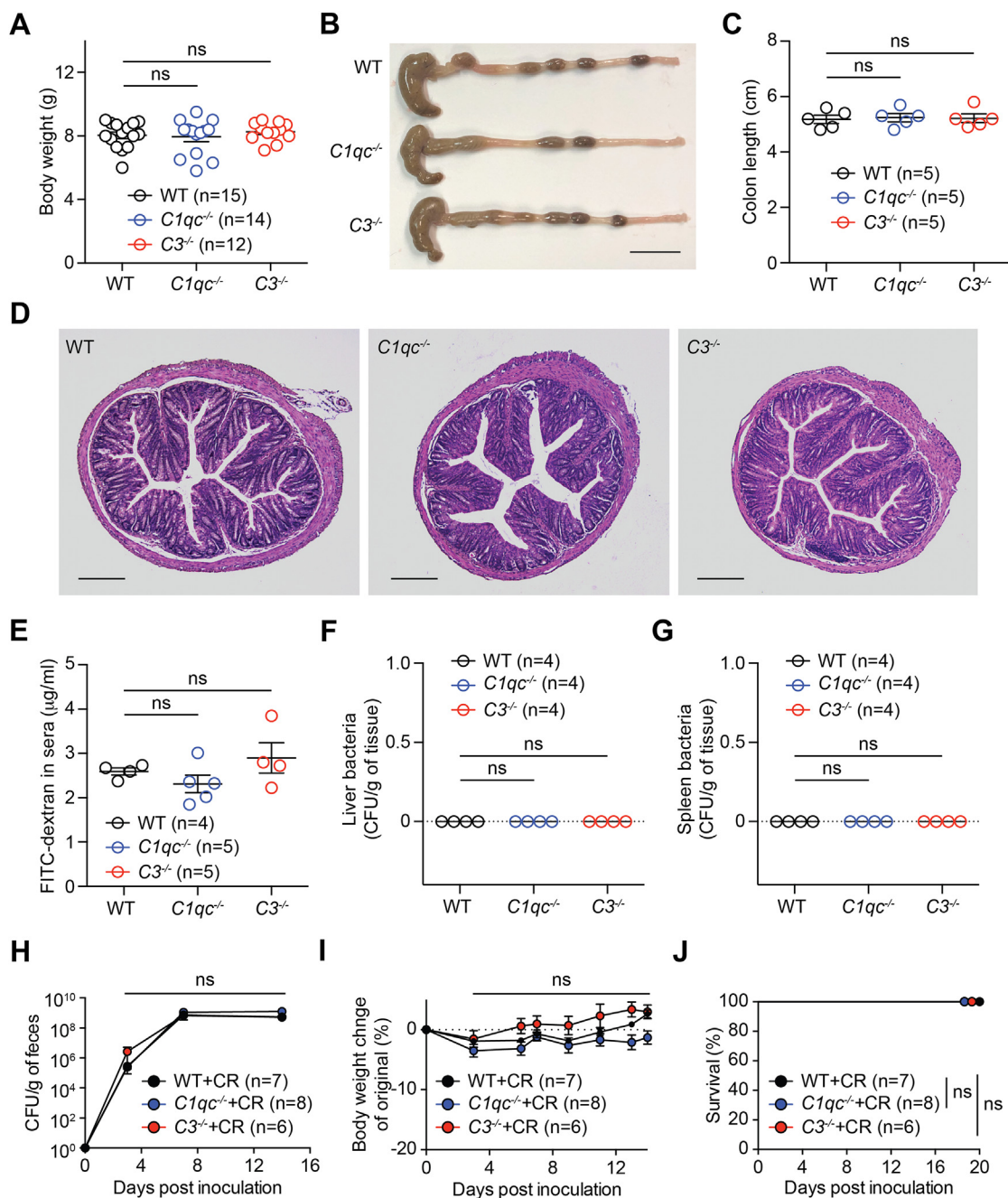


Figure S1. Complement-sufficient and -deficient mice are comparable in weaning stage without *Citrobacter rodentium* (CR) challenge and in adulthood with CR challenge, related to Figure 1

(A) Body weight of 21-day-old wild-type (WT) C57BL/6J, $C1qc^{-/-}$, and $C3^{-/-}$ mice.

(B and C) Representative macrographs (B) and lengths (C) of the colon derived from 21-day-old WT, $C1qc^{-/-}$, and $C3^{-/-}$ pups. Scale bars, 1 cm.

(D) Hematoxylin and eosin staining of colon sections derived from 21-day-old WT, $C1qc^{-/-}$, and $C3^{-/-}$ pups. Scale bars, 200 μ m.

(E) FITC-dextran concentrations in the sera of 21-day-old WT, $C1qc^{-/-}$, and $C3^{-/-}$ pups at 4 h post oral administration of FITC-dextran.

(legend continued on next page)

(F and G) Live bacterial burdens recovered from the liver (F) and the spleen (G) of 21-day-old WT, *C1qc*^{-/-}, and *C3*^{-/-} pups.

(H) Live *C. rodentium* (CR) burdens recovered from the fecal samples of 6- to 8-week-old WT, *C1qc*^{-/-}, and *C3*^{-/-} mice at indicated days post inoculation (dpi) with 2×10^9 CFUs of CR.

(I and J) Body weight changes (I) and survival (J) of 6- to 8-week-old WT, *C1qc*^{-/-}, and *C3*^{-/-} mice, infected with 2×10^9 CFUs of CR, at indicated dpi. Data are mean \pm SEM, with specific n numbers indicated, and representative of at least two independent experiments. ns, not significant.

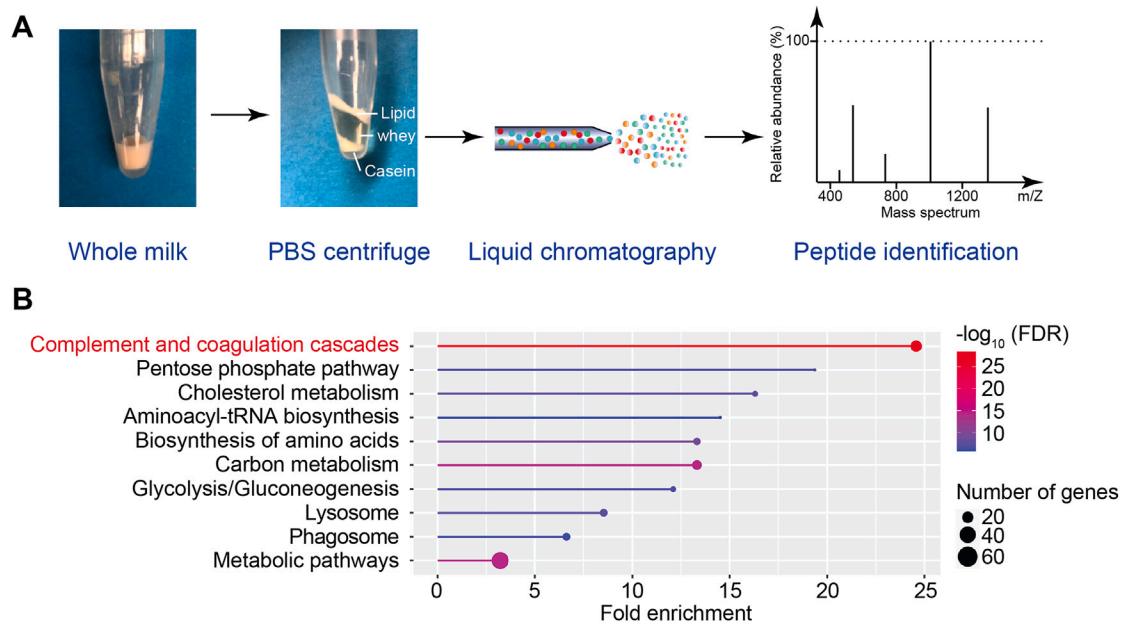


Figure S2. Complement components are among the most abundant proteins detected in wild-type C57BL/6J mouse whey, related to Figure 2

(A) Experimental scheme of mass spectrometry of whey proteins after centrifugation of whole milk derived from lactating wild-type (WT) C57BL/6J dams.
 (B) Functional gene ontology enrichment analysis of WT mouse whey proteins by the ShinyGO (v0.741). Shown is lollipop illustration of the top 10 Kyoto Encyclopedia of Genes and Genomes (KEGG) pathway categories, ranked by fold enrichment. Complement and coagulation cascades pathway is highlighted in red.

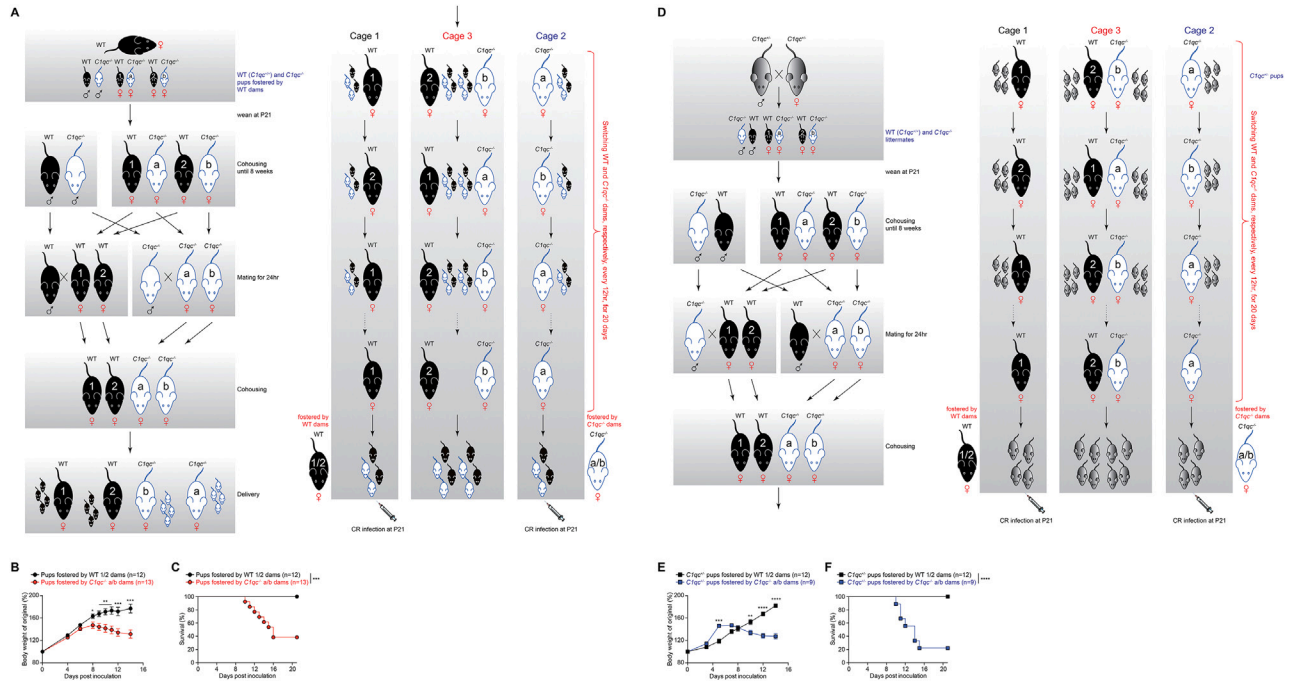


Figure S3. Complement in breast milk of cohoused dams protects weaning mice from lethal infection with *Citrobacter rodentium*, related to Figure 2

(A) Experimental scheme of dam cohousing strategy. Wild-type (WT) C57BL/6J (black, filled) and *C1qc*^{-/-} (blue, open) breeding pairs were synchronized to generate pups born on the same day. At the day of birth, WT and *C1qc*^{-/-} pups were identified and fostered by a WT dam. At post-natal day 21 (P21), WT females (1/2), and *C1qc*^{-/-} females (a/b), as well as WT and *C1qc*^{-/-} males, were separated and cohoused. At the age of 8 weeks, WT and *C1qc*^{-/-} mice were paired separately for mating; fertilized WT females (1/2) and *C1qc*^{-/-} females (a/b) were cohoused again until delivering pups. After delivery, 1/4 of the newborns (mixture of WT and *C1qc*^{-/-} pups) were fostered in cage 1 by WT dam (1) or in cage 2 by *C1qc*^{-/-} dam (a), while the other WT dam (2), the other *C1qc*^{-/-} dam (b), and the rest of the newborns (mixture of WT and *C1qc*^{-/-} pups) were cohoused in cage 3. Dams were switched between cage 1 and cage 3 for WT dams (1/2) and between cage 2 and cage 3 for *C1qc*^{-/-} dams (a/b), every 12 h, for 20 days. After 21 days of fostering, pups were separated from dams and subjected to oral inoculation with *Citrobacter rodentium* (CR).

(B and C) Body weight changes (B) and survival (C) of the pups fostered by the indicated dams at indicated days post inoculation (dpi) with 2×10^9 CFUs of CR. (D) Experimental scheme of littermate-breeding and dam cohousing strategies. WT (black, filled) and *C1qc*^{-/-} (blue, open) littermates generated from *C1qc*^{+/-} (gray, filled) heterozygous breeding pairs were identified and weaned at post-natal day 21 (P21). Female WT (1/2) and *C1qc*^{-/-} (a/b) littermates, as well as male WT and *C1qc*^{-/-} littermates, were separated and cohoused. At the age of 8 weeks, WT females (1/2) and *C1qc*^{-/-} females (a/b) were mated with *C1qc*^{-/-} male and *C1qc*^{-/-} females (a/b) were bred with WT male, respectively; fertilized WT females (1/2) and *C1qc*^{-/-} females (a/b) were cohoused again until delivering pups. After delivery, 1/4 of the newborn *C1qc*^{+/-} pups were fostered in cage 1 by WT dam (1) or in cage 2 by *C1qc*^{-/-} dam (a), while the other WT dam (2), the other *C1qc*^{-/-} dam (b), and the rest of the *C1qc*^{+/-} newborns were cohoused in cage 3. Dams were switched between cage 1 and cage 3 for WT dams (1/2) and between cage 2 and cage 3 for *C1qc*^{-/-} dams (a/b), every 12 h, for 20 days. After 21 days of cross-fostering, *C1qc*^{+/-} pups were separated from dams and subjected to oral inoculation with *Citrobacter rodentium* (CR).

(E and F) Body weight changes (E) and survival (F) of the *C1qc*^{+/-} pups fostered by the indicated dams at indicated dpi with 2×10^9 CFUs of CR.

Data are mean \pm SEM, with specific n numbers indicated, and are combined results from two independent experiments. ** p < 0.01, *** p < 0.001, and **** p < 0.0001.

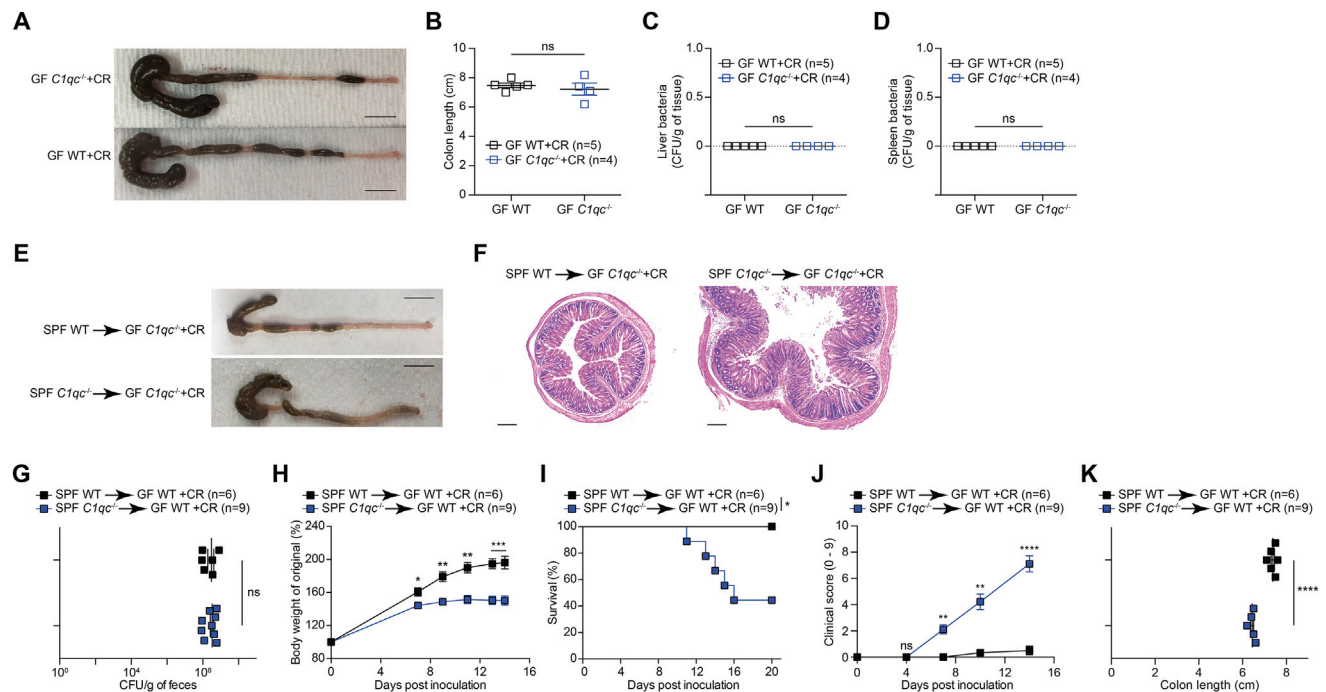


Figure S4. Gut microbiota confers the susceptibility of germ-free pups to *Citrobacter rodentium* infection, related to Figure 3

(A and B) Representative macrographs (A) and lengths (B) of the colon derived from 21-day-old germ-free (GF) wild-type (WT) C57BL/6J and *C1qc*^{-/-} pups at 14 days post inoculation (dpi) with 2×10^9 CFUs of *Citrobacter rodentium* (CR). Scale bars, 1 cm.

(C and D) CR burdens in the liver (C) and the spleen (D) derived from CR-infected GF WT and *C1qc*^{-/-} pups at 14 dpi.

(E and F) 21-day-old GF *C1qc*^{-/-} pups, reconstituted at post-natal day 17 (P17) with the cecal and colonic microbiota derived from P21 specific-pathogen-free (SPF) WT or *C1qc*^{-/-} pups, were orally infected with 2×10^9 CFUs of CR. Shown are representative photographs of the colon (E) and hematoxylin and eosin staining of colon sections (F) derived from indicated pups at 12 dpi. Scale bars, 1 cm (E) and 200 μm (F).

(G) Live CR recovered from the fecal samples of 21-day-old GF WT pups, reconstituted at P17 with the cecal and colonic microbiota derived from P21 SPF WT or *C1qc*^{-/-} pups, at 7 dpi with 2×10^9 CFUs of CR.

(H–J) Body weight changes (H), survival (I), and clinical scores (J) of 21-day-old GF WT pups, reconstituted and infected as in (G), at indicated dpi.

(K) Lengths of the colon derived from GF WT pups, reconstituted, and infected as in (G), at 12 dpi.

Data are mean ± SEM, with specific n numbers indicated. Data in (B)–(D) and (G)–(K) are combined results from two independent experiments. Data in (A), (E), and (F) are representative of three independent experiments. ns, not significant; * p < 0.05, ** p < 0.01, *** p < 0.001, and **** p < 0.0001.

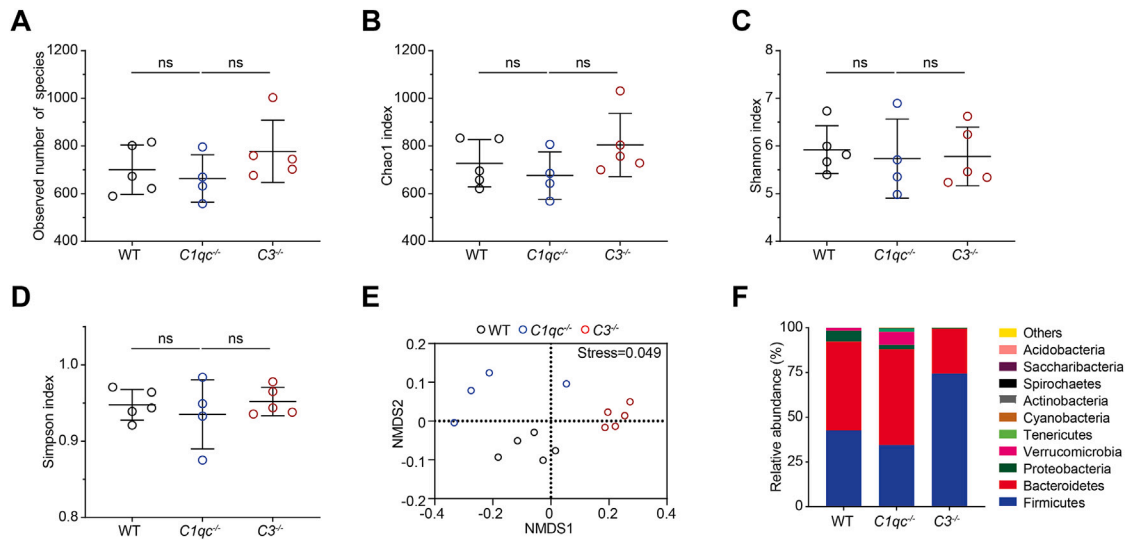


Figure S5. The gut microbiota of wild-type and complement-deficient pups are distinct, related to Figure 3

(A–D) Number of observed species (A), estimated community richness (B), Shannon index (C), and Simpson index (D) of the bacterial families, detected using 16S rRNA gene-based high-throughput sequencing, among the cecal and colonic contents derived from 21-day-old wild-type (WT) C57BL/6J ($n = 5$), $C1qc^{-/-}$ ($n = 4$), and $C3^{-/-}$ ($n = 5$) pups.

(E) Nonmetric multidimensional scaling (NMDS) plot of the bacterial families among the cecal and colonic contents derived from 21-day-old WT ($n = 5$), $C1qc^{-/-}$ ($n = 4$), and $C3^{-/-}$ ($n = 5$) pups. The analysis was based on ASVs from the sequences of the V4 regions of 16S rRNA.

(F) Relative abundance of the bacterial phyla among the cecal and colonic contents derived from 21-day-old WT ($n = 5$), $C1qc^{-/-}$ ($n = 4$), and $C3^{-/-}$ ($n = 5$) pups. Data are mean \pm SEM. Significant differences in (A)–(D) were evaluated by Kruskal-Wallis test. ns, not significant. Significant differences in each beta group in (E) were performed by PERMANOVA test. $p = 0.024$ for WT versus $C1qc^{-/-}$; $p = 0.007$ for WT versus $C3^{-/-}$; and $p = 0.006$ for $C1qc^{-/-}$ versus $C3^{-/-}$, respectively.

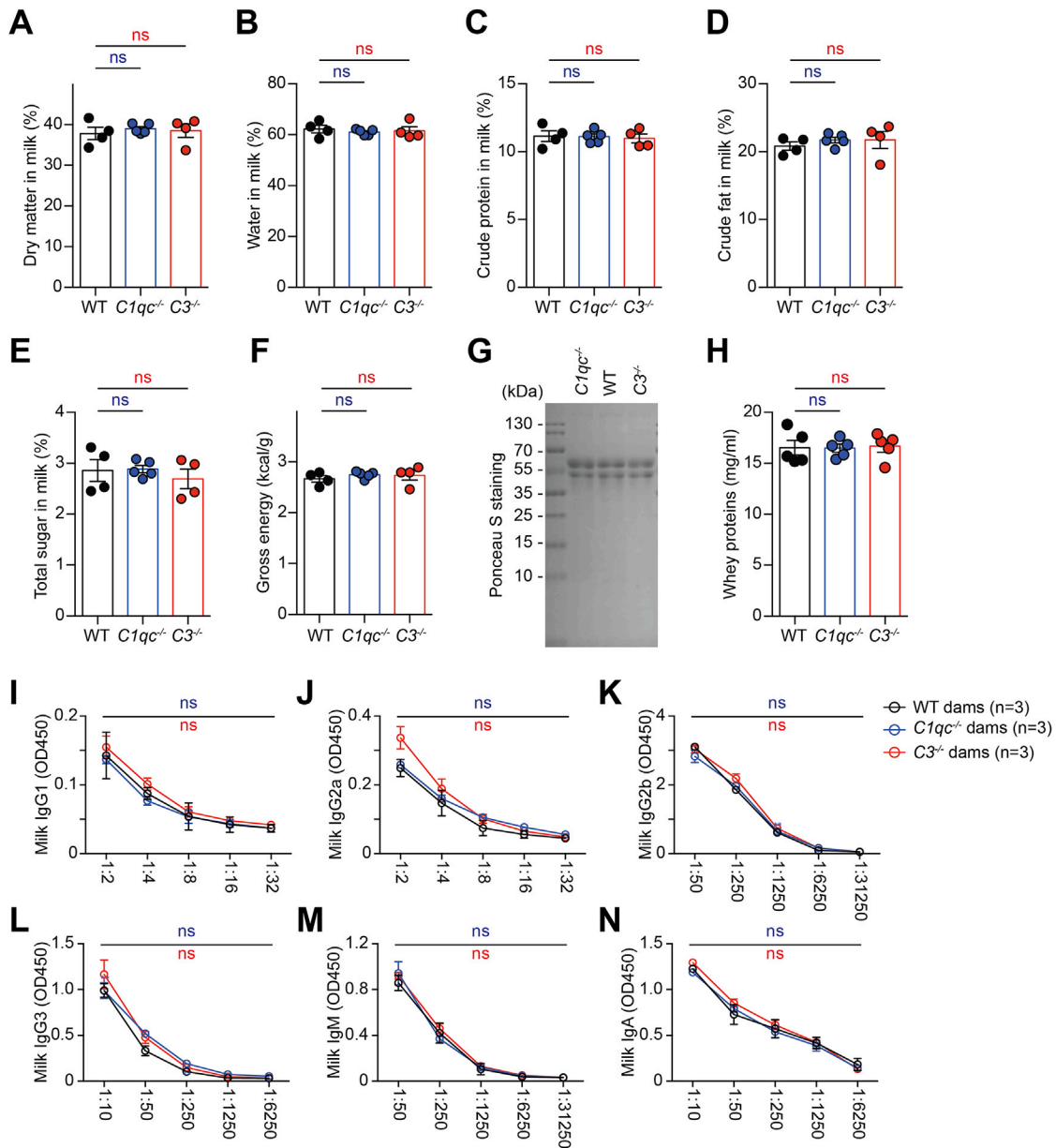


Figure S6. Breast milk compositions and produced antibodies in wild-type and complement-deficient dams are comparable, related to Figure 4

(A–F) Dry matter (A), water content (B), crude protein (C), crude fat (D), total sugar (E), and gross energy (F) of breast milk derived from lactating wild-type (WT) C57BL/6J, *C1qc*^{-/-}, and *C3*^{-/-} dams.

(G) Representative image of Ponceau S staining, following the SDS-PAGE separation, of whey proteins isolated from WT, *C1qc*^{-/-}, and *C3*^{-/-} dams.

(H) Protein concentrations of whey derived from WT, *C1qc*^{-/-}, and *C3*^{-/-} dams.

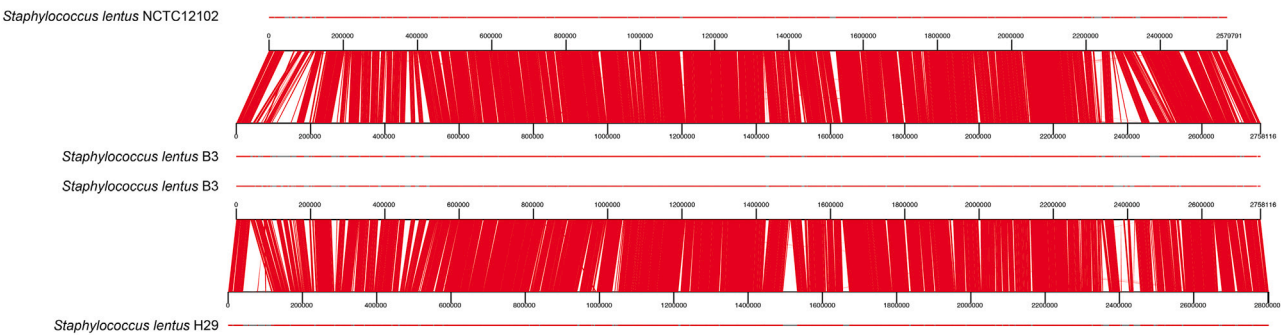
(I–N) Titers of indicated mouse immunoglobulin G1 (IgG1) (I), IgG2a (J), IgG2b (K), IgG3 (L), IgM (M), and IgA (N) in whey derived from lactating WT, *C1qc*^{-/-}, and *C3*^{-/-} dams.

Data are mean ± SEM, with specific n numbers indicated. Data in G are representative of three independent experiments. ns, not significant, for *C1qc*^{-/-} versus WT in blue and *C3*^{-/-} versus WT in red, respectively.

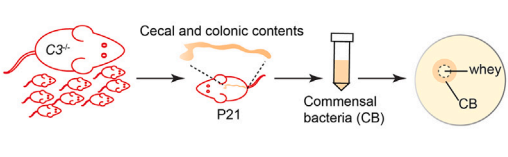
A

<i>Staphylococcus lentus</i> B3	TGCTTCTCTGATGTTAGCGGCGACGGGTGAGTAAACAGCTGGGTAACCTTACCTATAAGACTGGGTAACCTCGGGAAACCGGGGCTAAATACCGGATAATATATTGAACCCGATGGTTCAA	147
<i>Staphylococcus lentus</i> FJAT-hcl-24	TCCTTCTCTGATGTTAGCGGCGACGGGTGAGTAAACAGCTGGGTAACCTTACCTATAAGACTGGGTAACCTCGGGAAACCGGGGCTAAATACCGGATAATATATTGAACCCGATGGTTCAA	147
<i>Staphylococcus lentus</i> H2R31	TGCTTCTCTGATGTTAGCGGCGACGGGTGAGTAAACAGCTGGGTAACCTTACCTATAAGACTGGGTAACCTCGGGAAACCGGGGCTAAATACCGGATAATATATTGAACCCGATGGTTCAA	148
<i>Staphylococcus lentus</i> HSL4	TGCTTCTCTGATGTTAGCGGCGACGGGTGAGTAAACAGCTGGGTAACCTTACCTATAAGACTGGGTAACCTCGGGAAACCGGGGCTAAATACCGGATAATATATTGAACCCGATGGTTCAA	154
<i>Staphylococcus lentus</i> RCB297	TGCTTCTCTGATGTTAGCGGCGACGGGTGAGTAAACAGCTGGGTAACCTTACCTATAAGACTGGGTAACCTCGGGAAACCGGGGCTAAATACCGGATAATATATTGAACCCGATGGTTCAA	154
<i>Staphylococcus lentus</i> RCB409	TGCTTCTCTGATGTTAGCGGCGACGGGTGAGTAAACAGCTGGGTAACCTTACCTATAAGACTGGGTAACCTCGGGAAACCGGGGCTAAATACCGGATAATATATTGAACCCGATGGTTCAA	174
<i>Staphylococcus lentus</i> B3	TGTTGAAAGACGGTTTCGGCTGTCACTTATAGATGACCCCGGCCGCTATAGCTAGTTGGTAAAGTAAACCGCTTACCAAGGCAACGATACGTAGCCGACCTGAGAGGGTGTATGGGCCACA	267
<i>Staphylococcus lentus</i> FJAT-hcl-24	TGTTGAAAGACGGTTTCGGCTGTCACTTATAGATGACCCCGGCCGCTATAGCTAGTTGGTAAAGTAAACCGCTTACCAAGGCAACGATACGTAGCCGACCTGAGAGGGTGTATGGGCCACA	267
<i>Staphylococcus lentus</i> H2R31	TGTTGAAAGACGGTTTCGGCTGTCACTTATAGATGACCCCGGCCGCTATAGCTAGTTGGTAAAGTAAACCGCTTACCAAGGCAACGATACGTAGCCGACCTGAGAGGGTGTATGGGCCACA	263
<i>Staphylococcus lentus</i> HSL4	TGTTGAAAGACGGTTTCGGCTGTCACTTATAGATGACCCCGGCCGCTATAGCTAGTTGGTAAAGTAAACCGCTTACCAAGGCAACGATACGTAGCCGACCTGAGAGGGTGTATGGGCCACA	290
<i>Staphylococcus lentus</i> RCB297	TGTTGAAAGACGGTTTCGGCTGTCACTTATAGATGACCCCGGCCGCTATAGCTAGTTGGTAAAGTAAACCGCTTACCAAGGCAACGATACGTAGCCGACCTGAGAGGGTGTATGGGCCACA	294
<i>Staphylococcus lentus</i> RCB409	TGTTGAAAGACGGTTTCGGCTGTCACTTATAGATGACCCCGGCCGCTATAGCTAGTTGGTAAAGTAAACCGCTTACCAAGGCAACGATACGTAGCCGACCTGAGAGGGTGTATGGGCCACA	274
<i>Staphylococcus lentus</i> B3	CTGGAACTGAGACAGCTCCAGACTCCTACCGGAGGACAGCAGTAGGAAATCTCCGCAATGGGCGAAAGCCTGACGGGCAACCGCCGCTGAGTGTAGAGGCTTTAGGACTGTAATAACT	387
<i>Staphylococcus lentus</i> FJAT-hcl-24	CTGGAACTGAGACAGCTCCAGACTCCTACCGGAGGACAGCAGTAGGAAATCTCCGCAATGGGCGAAAGCCTGACGGGCAACCGCCGCTGAGTGTAGAGGCTTTAGGACTGTAATAACT	387
<i>Staphylococcus lentus</i> H2R31	CTGGAACTGAGACAGCTCCAGACTCCTACCGGAGGACAGCAGTAGGAAATCTCCGCAATGGGCGAAAGCCTGACGGGCAACCGCCGCTGAGTGTAGAGGCTTTAGGACTGTAATAACT	393
<i>Staphylococcus lentus</i> HSL4	CTGGAACTGAGACAGCTCCAGACTCCTACCGGAGGACAGCAGTAGGAAATCTCCGCAATGGGCGAAAGCCTGACGGGCAACCGCCGCTGAGTGTAGAGGCTTTAGGACTGTAATAACT	384
<i>Staphylococcus lentus</i> RCB297	CTGGAACTGAGACAGCTCCAGACTCCTACCGGAGGACAGCAGTAGGAAATCTCCGCAATGGGCGAAAGCCTGACGGGCAACCGCCGCTGAGTGTAGAGGCTTTAGGACTGTAATAACT	384
<i>Staphylococcus lentus</i> RCB409	CTGGAACTGAGACAGCTCCAGACTCCTACCGGAGGACAGCAGTAGGAAATCTCCGCAATGGGCGAAAGCCTGACGGGCAACCGCCGCTGAGTGTAGAGGCTTTAGGACTGTAATAACT	414
<i>Staphylococcus lentus</i> B3	CTGTGTTAGGGAAGAACAAATTTGTTAGTAACGAAACAGCTTTCGCGTACTTAAACGAAAGCCAGCGCTAACCTACGTGCCAGCAGCCGGTAAATACGTAGTGGCAAGCGTTATC	507
<i>Staphylococcus lentus</i> FJAT-hcl-24	CTGTGTTAGGGAAGAACAAATTTGTTAGTAACGAAACAGCTTTCGCGTACTTAAACGAAAGCCAGCGCTAACCTACGTGCCAGCAGCCGGTAAATACGTAGTGGCAAGCGTTATC	507
<i>Staphylococcus lentus</i> H2R31	CTGTGTTAGGGAAGAACAAATTTGTTAGTAACGAAACAGCTTTCGCGTACTTAAACGAAAGCCAGCGCTAACCTACGTGCCAGCAGCCGGTAAATACGTAGTGGCAAGCGTTATC	420
<i>Staphylococcus lentus</i> HSL4	CTGTGTTAGGGAAGAACAAATTTGTTAGTAACGAAACAGCTTTCGCGTACTTAAACGAAAGCCAGCGCTAACCTACGTGCCAGCAGCCGGTAAATACGTAGTGGCAAGCGTTATC	540
<i>Staphylococcus lentus</i> RCB297	CTGTGTTAGGGAAGAACAAATTTGTTAGTAACGAAACAGCTTTCGCGTACTTAAACGAAAGCCAGCGCTAACCTACGTGCCAGCAGCCGGTAAATACGTAGTGGCAAGCGTTATC	514
<i>Staphylococcus lentus</i> RCB409	CTGTGTTAGGGAAGAACAAATTTGTTAGTAACGAAACAGCTTTCGCGTACTTAAACGAAAGCCAGCGCTAACCTACGTGCCAGCAGCCGGTAAATACGTAGTGGCAAGCGTTATC	514
<i>Staphylococcus lentus</i> B3	CGGAATTTTGGCGTAAAGCGCGCTAGGCGGTTTCTTAAGTCTGATGTGAAAGCCACGGCTCAACCGTGGAGGGTCAATTGAAACTGGGAACTTGAGTCGAGAAGAGGAGAGTGGGA	623
<i>Staphylococcus lentus</i> FJAT-hcl-24	CGGAATTTTGGCGTAAAGCGCGCTAGGCGGTTTCTTAAGTCTGATGTGAAAGCCACGGCTCAACCGTGGAGGGTCAATTGAAACTGGGAACTTGAGTCGAGAAGAGGAGAGTGGGA	623
<i>Staphylococcus lentus</i> H2R31	CGGAATTTTGGCGTAAAGCGCGCTAGGCGGTTTCTTAAGTCTGATGTGAAAGCCACGGCTCAACCGTGGAGGGTCAATTGAAACTGGGAACTTGAGTCGAGAAGAGGAGAGTGGGA	627
<i>Staphylococcus lentus</i> HSL4	CGGAATTTTGGCGTAAAGCGCGCTAGGCGGTTTCTTAAGTCTGATGTGAAAGCCACGGCTCAACCGTGGAGGGTCAATTGAAACTGGGAACTTGAGTCGAGAAGAGGAGAGTGGGA	660
<i>Staphylococcus lentus</i> RCB297	CGGAATTTTGGCGTAAAGCGCGCTAGGCGGTTTCTTAAGTCTGATGTGAAAGCCACGGCTCAACCGTGGAGGGTCAATTGAAACTGGGAACTTGAGTCGAGAAGAGGAGAGTGGGA	660
<i>Staphylococcus lentus</i> RCB409	CGGAATTTTGGCGTAAAGCGCGCTAGGCGGTTTCTTAAGTCTGATGTGAAAGCCACGGCTCAACCGTGGAGGGTCAATTGAAACTGGGAACTTGAGTCGAGAAGAGGAGAGTGGGA	654
<i>Staphylococcus lentus</i> B3	ATTTCCATGTTAGCGGTAATTCGCGAGAGATATGGAGGAACCCAGTGGCAAGCCAGCGCTCTCTGCTGTGTAACGACCGTGTATGCGAAAGCGTGGGATCAACACAGGATATAGATAC	747
<i>Staphylococcus lentus</i> FJAT-hcl-24	ATTTCCATGTTAGCGGTAATTCGCGAGAGATATGGAGGAACCCAGTGGCAAGCCAGCGCTCTCTGCTGTGTAACGACCGTGTATGCGAAAGCGTGGGATCAACACAGGATATAGATAC	747
<i>Staphylococcus lentus</i> H2R31	ATTTCCATGTTAGCGGTAATTCGCGAGAGATATGGAGGAACCCAGTGGCAAGCCAGCGCTCTCTGCTGTGTAACGACCGTGTATGCGAAAGCGTGGGATCAACACAGGATATAGATAC	743
<i>Staphylococcus lentus</i> HSL4	ATTTCCATGTTAGCGGTAATTCGCGAGAGATATGGAGGAACCCAGTGGCAAGCCAGCGCTCTCTGCTGTGTAACGACCGTGTATGCGAAAGCGTGGGATCAACACAGGATATAGATAC	780
<i>Staphylococcus lentus</i> RCB297	ATTTCCATGTTAGCGGTAATTCGCGAGAGATATGGAGGAACCCAGTGGCAAGCCAGCGCTCTCTGCTGTGTAACGACCGTGTATGCGAAAGCGTGGGATCAACACAGGATATAGATAC	754
<i>Staphylococcus lentus</i> RCB409	ATTTCCATGTTAGCGGTAATTCGCGAGAGATATGGAGGAACCCAGTGGCAAGCCAGCGCTCTCTGCTGTGTAACGACCGTGTATGCGAAAGCGTGGGATCAACACAGGATATAGATAC	774
<i>Staphylococcus lentus</i> B3	CCGTGTAGTCCACCGCTAAACGATGAGTGTCTAAGTGTAGGAGGGTTTCGCGCCCTTAGTGTCTGACGCTAACGATTAAGCACTCCGCTGGGGAGTACGACCGCAGGTTGAAACTCAA	867
<i>Staphylococcus lentus</i> FJAT-hcl-24	CCGTGTAGTCCACCGCTAAACGATGAGTGTCTAAGTGTAGGAGGGTTTCGCGCCCTTAGTGTCTGACGCTAACGATTAAGCACTCCGCTGGGGAGTACGACCGCAGGTTGAAACTCAA	863
<i>Staphylococcus lentus</i> H2R31	CCGTGTAGTCCACCGCTAAACGATGAGTGTCTAAGTGTAGGAGGGTTTCGCGCCCTTAGTGTCTGACGCTAACGATTAAGCACTCCGCTGGGGAGTACGACCGCAGGTTGAAACTCAA	900
<i>Staphylococcus lentus</i> HSL4	CCGTGTAGTCCACCGCTAAACGATGAGTGTCTAAGTGTAGGAGGGTTTCGCGCCCTTAGTGTCTGACGCTAACGATTAAGCACTCCGCTGGGGAGTACGACCGCAGGTTGAAACTCAA	874
<i>Staphylococcus lentus</i> RCB297	CCGTGTAGTCCACCGCTAAACGATGAGTGTCTAAGTGTAGGAGGGTTTCGCGCCCTTAGTGTCTGACGCTAACGATTAAGCACTCCGCTGGGGAGTACGACCGCAGGTTGAAACTCAA	894
<i>Staphylococcus lentus</i> RCB409	CCGTGTAGTCCACCGCTAAACGATGAGTGTCTAAGTGTAGGAGGGTTTCGCGCCCTTAGTGTCTGACGCTAACGATTAAGCACTCCGCTGGGGAGTACGACCGCAGGTTGAAACTCAA	894
<i>Staphylococcus lentus</i> B3	AGGAATGACGGGGACCCGACAAAGCGGTGGAGCATGTGGTTTAAATTCGAAGCAACCGGAAGAACCTTACCAAATCTTGACATCTTTGACCGCTCTAGAGATAGAGTTTCCCTTCGG	987
<i>Staphylococcus lentus</i> FJAT-hcl-24	AGGAATGACGGGGACCCGACAAAGCGGTGGAGCATGTGGTTTAAATTCGAAGCAACCGGAAGAACCTTACCAAATCTTGACATCTTTGACCGCTCTAGAGATAGAGTTTCCCTTCGG	987
<i>Staphylococcus lentus</i> H2R31	AGGAATGACGGGGACCCGACAAAGCGGTGGAGCATGTGGTTTAAATTCGAAGCAACCGGAAGAACCTTACCAAATCTTGACATCTTTGACCGCTCTAGAGATAGAGTTTCCCTTCGG	1020
<i>Staphylococcus lentus</i> HSL4	AGGAATGACGGGGACCCGACAAAGCGGTGGAGCATGTGGTTTAAATTCGAAGCAACCGGAAGAACCTTACCAAATCTTGACATCTTTGACCGCTCTAGAGATAGAGTTTCCCTTCGG	994
<i>Staphylococcus lentus</i> RCB297	AGGAATGACGGGGACCCGACAAAGCGGTGGAGCATGTGGTTTAAATTCGAAGCAACCGGAAGAACCTTACCAAATCTTGACATCTTTGACCGCTCTAGAGATAGAGTTTCCCTTCGG	1014
<i>Staphylococcus lentus</i> RCB409	AGGAATGACGGGGACCCGACAAAGCGGTGGAGCATGTGGTTTAAATTCGAAGCAACCGGAAGAACCTTACCAAATCTTGACATCTTTGACCGCTCTAGAGATAGAGTTTCCCTTCGG	1114
<i>Staphylococcus lentus</i> B3	GGGACAAAGTACAGGTGGTGCATGTTGCTGCTCAGCTCTGTCGTGAGATGTTGGGTTAAGTCCCGCAACGAGCGCAACCCCTTAAGCTTAGTTGCCATCATTAAAGTTGGGCACCTTAGG	1107
<i>Staphylococcus lentus</i> FJAT-hcl-24	GGGACAAAGTACAGGTGGTGCATGTTGCTGCTCAGCTCTGTCGTGAGATGTTGGGTTAAGTCCCGCAACGAGCGCAACCCCTTAAGCTTAGTTGCCATCATTAAAGTTGGGCACCTTAGG	1103
<i>Staphylococcus lentus</i> H2R31	GGGACAAAGTACAGGTGGTGCATGTTGCTGCTCAGCTCTGTCGTGAGATGTTGGGTTAAGTCCCGCAACGAGCGCAACCCCTTAAGCTTAGTTGCCATCATTAAAGTTGGGCACCTTAGG	1140
<i>Staphylococcus lentus</i> HSL4	GGGACAAAGTACAGGTGGTGCATGTTGCTGCTCAGCTCTGTCGTGAGATGTTGGGTTAAGTCCCGCAACGAGCGCAACCCCTTAAGCTTAGTTGCCATCATTAAAGTTGGGCACCTTAGG	1140
<i>Staphylococcus lentus</i> RCB297	GGGACAAAGTACAGGTGGTGCATGTTGCTGCTCAGCTCTGTCGTGAGATGTTGGGTTAAGTCCCGCAACGAGCGCAACCCCTTAAGCTTAGTTGCCATCATTAAAGTTGGGCACCTTAGG	1114
<i>Staphylococcus lentus</i> RCB409	GGGACAAAGTACAGGTGGTGCATGTTGCTGCTCAGCTCTGTCGTGAGATGTTGGGTTAAGTCCCGCAACGAGCGCAACCCCTTAAGCTTAGTTGCCATCATTAAAGTTGGGCACCTTAGG	1134

B



C



D

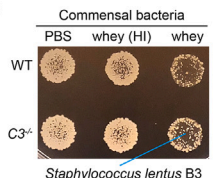


Figure S7. Complement in mouse breast milk whey kills *Staphylococcus lentus* B3 strain, related to Figure 4
 (A) Alignment of the 16S rRNA gene sequences of *Staphylococcus lentus* B3 and five *S. lentus* strains from the NCBI database.
 (B) Linear comparison of *S. lentus* B3 (middle) with complete genomes of *S. lentus* strains NCTC12102 (top) and H29 (bottom). The origin of H29 genome (CP059679) was manually adjusted based on that of NCTC12102 (UHDR0100002) for better visualization. Red parallelograms within each genome pair indicate the locations of homologous genomic sequences. The horizontal bars denote the shared backbone (red) and genomic island (gray) of each genome.
 (C) Schematic of the experimental workflow. Cecal and colonic contents from a P21 mouse are used to establish a community of commensal bacteria (CB) in a C3- mouse. *Staphylococcus lentus* B3 is then isolated from this community.
 (D) Spot assay showing the growth of *Staphylococcus lentus* B3 on different media. The top row shows growth on Commensal bacteria, PBS, whey (HI), and whey. The bottom row shows growth on the same media for the C3- strain. The B3 strain shows robust growth on whey, while the C3- strain shows reduced growth.

(legend continued on next page)

(C and D) Experimental scheme (C) and representative macrographs (D) of bactericidal assays on LB agar plates using wild-type (WT) C57BL/6J and $C3^{-/-}$ mouse whey to kill cultivable commensal bacteria (CB) derived from the $C3^{-/-}$ pups at post-natal day 21 (P21), with PBS and heat-inactivated (HI) whey as negative controls. Indicated is one species, *Staphylococcus lentus* B3 strain, isolated from the cultivable CB of $C3^{-/-}$ pups. Data are mean \pm SEM, with specific n numbers indicated. Data in (D) are representative of three independent experiments.

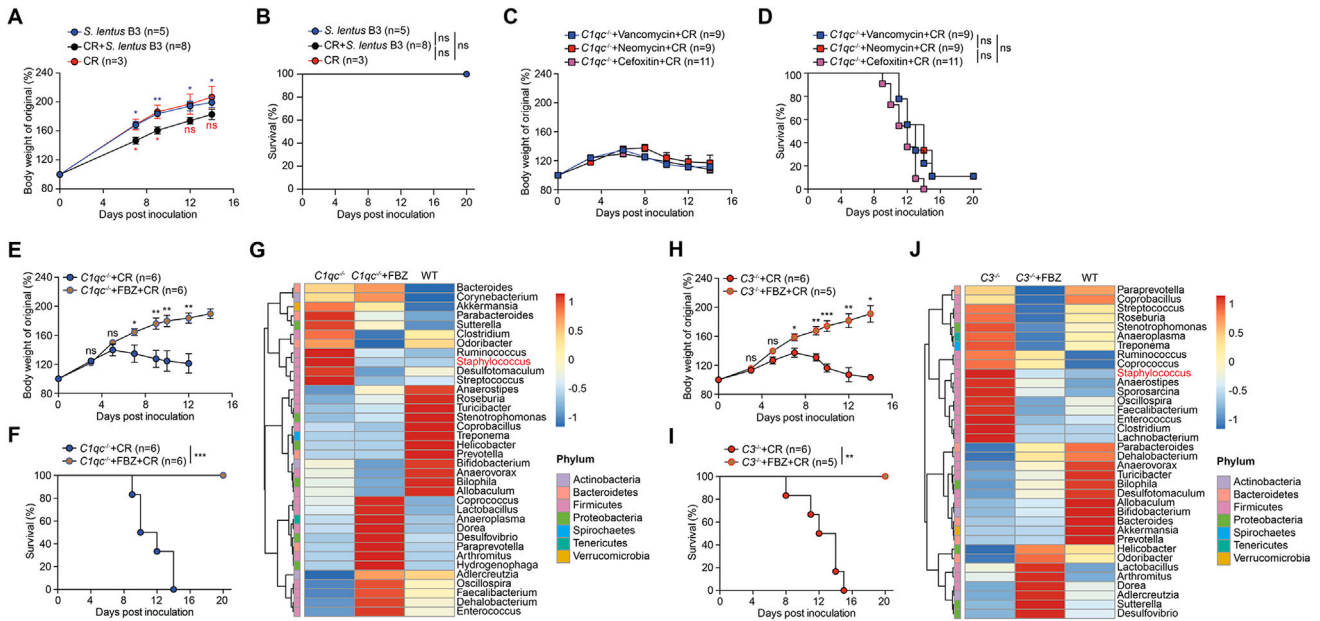


Figure S8. *Staphylococcus* abundance is associated with the susceptibility of weaning mice to *Citrobacter rodentium* infection, related to Figure 4

(A and B) Body weight changes (A) and survival (B) of 21-day-old germ-free (GF) *C1qc*^{-/-} pups at indicated days post inoculation (dpi) with 1 × 10⁹ CFUs of *Citrobacter rodentium* (CR) alone, 1 × 10⁹ CFUs of *S. lentus* B3 alone, or mixture of CR and *S. lentus* B3 (1:1 ratio, 1 × 10⁹ CFUs each).

(C and D) Body weight changes (C) and survival (D) of 21-day-old specific-pathogen-free (SPF) *C1qc*^{-/-} pups, fostered by the *C1qc*^{-/-} dams fed with sterile drinking water containing indicated antibiotics during lactation period, at indicated dpi with 2 × 10⁹ CFUs of CR.

(E and F) Body weight changes (E) and survival (F) of 21-day-old SPF *C1qc*^{-/-} pups, fostered by the *C1qc*^{-/-} dams fed with a diet containing therapeutic level of fenbendazole (FBZ, 150 ppm) during lactation period, at indicated dpi with 2 × 10⁹ CFUs of CR.

(G) Species abundance heatmap of the dominant 36 genera detected using 16S rRNA gene-based sequencing among the cecal and colonic contents derived from 21-day-old *C1qc*^{-/-} pups fostered by *C1qc*^{-/-} dams (n = 4), *C1qc*^{-/-} pups fostered by the FBZ-treated *C1qc*^{-/-} dams (n = 5), and wild-type (WT) pups fostered by WT dams (n = 5).

(H and I) Body weight changes (H) and survival (I) of 21-day-old SPF *C3*^{-/-} pups, fostered by the *C3*^{-/-} dams fed with a diet containing therapeutic level of fenbendazole (FBZ, 150 ppm) during lactation period, at indicated dpi with 2 × 10⁹ CFUs of CR.

(J) Species abundance heatmap of the dominant 36 genera detected using 16S rRNA gene-based sequencing among the cecal and colonic contents derived from 21-day-old *C3*^{-/-} pups fostered by *C3*^{-/-} dams (n = 4), *C3*^{-/-} pups fostered by the FBZ-treated *C3*^{-/-} dams (n = 4), and WT pups fostered by WT dams (n = 5).

Data are mean ± SEM, with specific n numbers indicated. Data in (A)–(F), (H), and (I) combined results from at least two independent experiments. ns, not significant; * p < 0.05, ** p < 0.01, and *** p < 0.001. ns, not significant; * p < 0.05, and ** p < 0.01, for mixture (CR + *S. lentus* B3) versus *S. lentus* B3 alone in blue and (CR + *S. lentus* B3) versus CR alone in red, respectively (A).

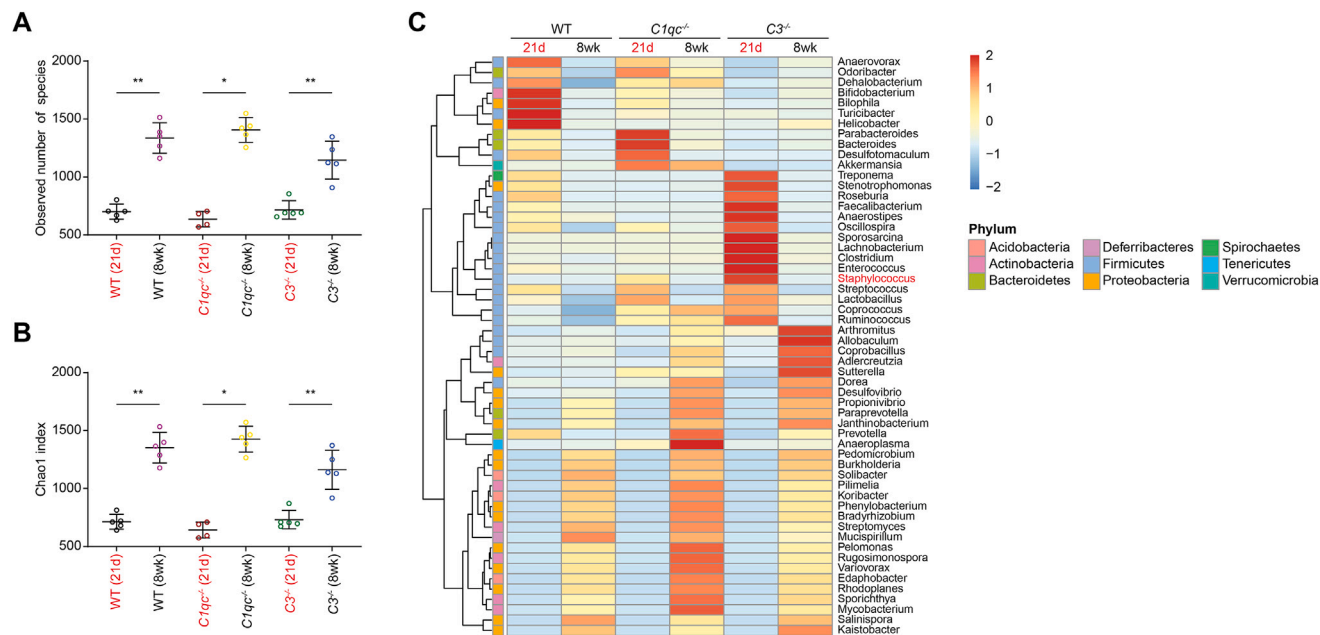


Figure S9. Gut commensal microbiota compositions in weaning and adult complement-sufficient and -deficient mice, related to Figure 4 (A and B) Number of observed species (A) and estimated community richness (B) of the bacterial families, detected using 16S rRNA gene-based high-throughput sequencing, among the cecal and colonic contents derived from 21-day-old wild-type (WT) ($n = 5$), $C1qc^{-/-}$ ($n = 4$), and $C3^{-/-}$ ($n = 5$) pups, as well as 8-week-old WT ($n = 5$), $C1qc^{-/-}$ ($n = 5$), and $C3^{-/-}$ ($n = 5$) adult mice. (C) Species abundance heatmap of the dominant 56 genera among the cecal and colonic contents derived from 21 days WT ($n = 5$), $C1qc^{-/-}$ ($n = 4$), and $C3^{-/-}$ ($n = 5$) pups, as well as 8 weeks WT ($n = 5$), $C1qc^{-/-}$ ($n = 5$), and $C3^{-/-}$ ($n = 5$) adult mice. Data are mean \pm SEM. * $p < 0.05$ and ** $p < 0.01$.

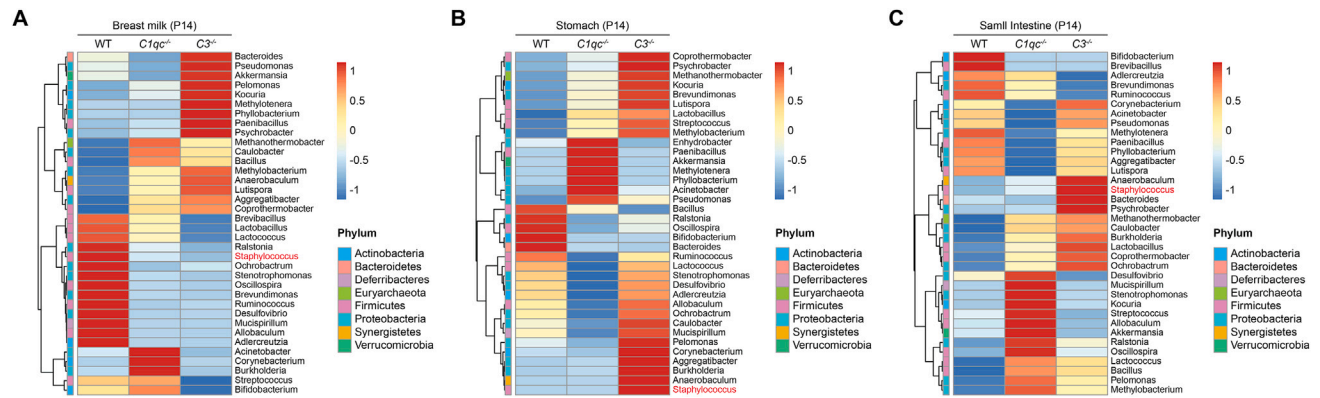


Figure S10. Microbiota compositions in the breast milk of dams and the stomach, the small intestine of 14-day-old suckling pups, related to Figure 4

(A) Species abundance heatmap of the dominant 36 genera detected using 16S rRNA gene-based high-throughput sequencing among the breast milk derived from wild-type (WT) C57BL/6J (n = 4), *C1qc*^{-/-} (n = 5), and *C3*^{-/-} (n = 4) dams, at post-natal day 14 (P14).

(B and C) Species abundance heatmap of the dominant 36 genera detected using 16S rRNA gene-based high-throughput sequencing among the stomach (B) and small intestine (C) contents derived from WT (n = 5), *C1qc*^{-/-} (n = 5), and *C3*^{-/-} (n = 5) pups at post-natal day 14 (P14).

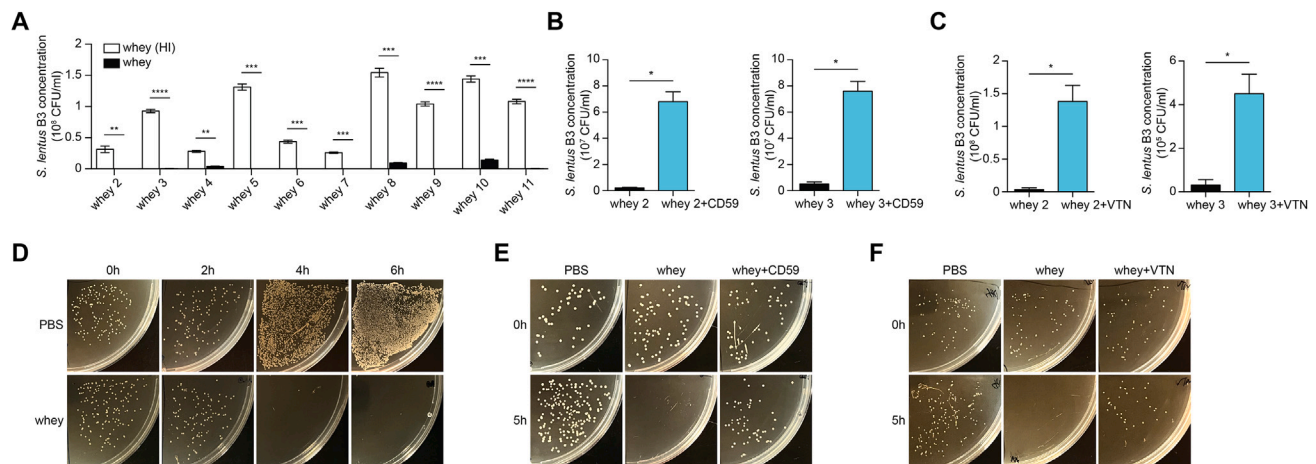


Figure S11. Human whey kills *Staphylococcus lentus* B3 in a complement dependent manner, related to Figure 4

(A) Human whey bactericidal assays using *Staphylococcus lentus* B3 cultured in LB medium, supplemented with regular or heat-inactivated (HI) human whey samples 2–11. After 16-h culture with shaking, the indicated *S. lentus* B3 cultures were serially diluted and spotted on LB agar plates to determine CFUs. Shown are the concentrations of live *S. lentus* B3 in indicated LB media.

(B and C) Human whey bactericidal assays using *S. lentus* B3 cultured in LB medium, as in (A). Shown are the concentrations of live *S. lentus* B3 in LB medium supplemented with human whey samples 2 and 3 in the presence and absence of CD59 (B) or vitronectin (VTN) (C).

(D–F) Time-kill kinetics assays using *S. lentus* B3 cultured in LB medium, supplemented with PBS or human whey (D) in the presence and absence of CD59 (E) or VTN (F). At each indicated time point, 100 μ L *S. lentus* B3 culture was plated on LB agar plates. Shown are representative images of LB plates after overnight culture.

Data are mean \pm SEM and representative of three independent experiments. * $p < 0.05$, ** $p < 0.01$, *** $p < 0.001$, and **** $p < 0.0001$.

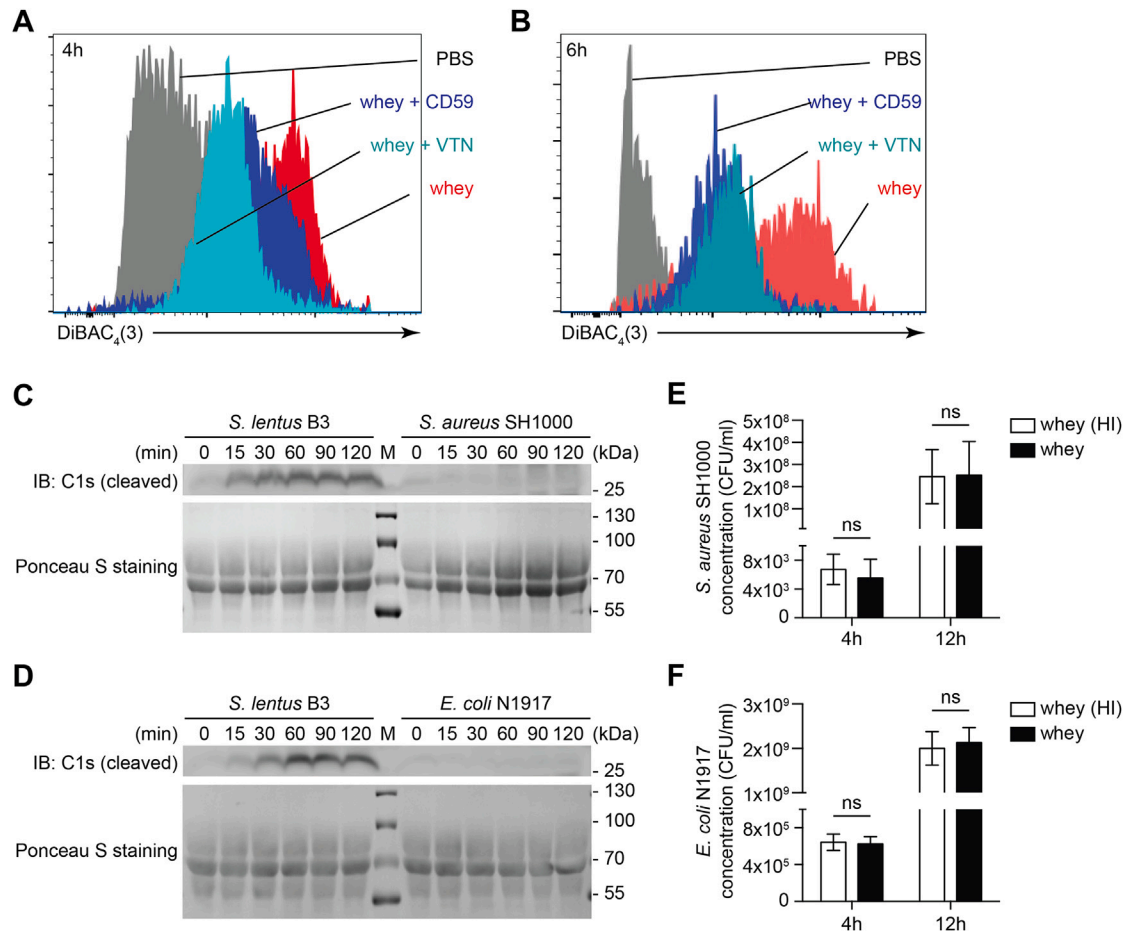


Figure S12. *Staphylococcus lentus* B3 triggers C1s activation in human whey, where complement disrupts bacterial membrane potential in CD59- and vitronectin-dependent manners, related to Figure 5

(A and B) Representative histograms of DiBAC₄(3) fluorescence on *Staphylococcus lentus* B3, following incubation with PBS or human whey, supplemented with CD59 or vitronectin (VTN) for 4 h (A) or 6 h (B), analyzed by flow cytometry.

(C and D) Human whey and *S. lentus* B3, *S. aureus* SH1000 (C), or *Escherichia coli* Nissle 1917 (*E. coli* N1917) (D) culture were incubated for indicated time periods, followed by SDS-PAGE separation. The membrane was subjected to Ponceau S staining or immunoblot (IB) for cleaved C1s proteins.

(E and F) Human whey bactericidal assays using *S. aureus* SH1000 (E) or *E. coli* N1917 (F) cultured in LB medium, supplemented with regular or heat-inactivated (HI) human whey. After 4- and 12-h culture with shaking, *S. aureus* SH1000 or *E. coli* N1917 cultures were serially diluted and spotted on LB agar plates to determine CFUs. Shown are the concentrations of live *S. aureus* SH1000 or *E. coli* N1917 in indicated LB media.

Data in (A)–(D) are representative of at least two independent experiments. Data in (E) and (F) are mean ± SEM and representative of three independent experiments. ns, not significant.